ISTANBUL TECHNICAL UNIVERSITY ★ GRADUATE SCHOOL OF SCIENCE ENGINEERING AND TECHNOLOGY

OPTIMIZATION OF DESIGN AND CONTROL PARAMETERS FOR AN ELECTRICALLY-PROPELLED AERIAL VEHICLE USING THE ENERGY APPROACH

M.Sc. THESIS

Ibrahim CICEK

Department of Aeronautical and Astronautical Engineering

Aeronautical & Astronautical Engineering Graduate Programme

JULY 2020

ISTANBUL TECHNICAL UNIVERSITY ★ GRADUATE SCHOOL OF SCIENCE ENGINEERING AND TECHNOLOGY

OPTIMIZATION OF DESIGN AND CONTROL PARAMETERS FOR AN ELECTRICALLY-PROPELLED AERIAL VEHICLE USING THE ENERGY APPROACH

M.Sc. THESIS

Ibrahim CICEK
(511171114)

Department of Aeronautical and Astronautical Engineering

Aeronautical & Astronautical Engineering Graduate Programme

Thesis Advisor: Prof. Dr. Melike NIKBAY

JULY 2020

İSTANBUL TEKNİK ÜNİVERSİTESİ ★ FEN BİLİMLERİ ENSTİTÜSÜ

ELEKTRİKSEL TAHRİKLİ BİR HAVA ARACININ ENERJİ YAKLAŞIMIYLA TASARIM VE KONTROL PARAMETRELERİ OPTİMİZASYONU

YÜKSEK LİSANS TEZİ

İbrahim ÇİÇEK
(511171114)

Uçak ve Uzay Mühendisliği Anabilim Dalı

Uçak ve Uzay Mühendisliği Yüksek Lisans Programı

Tez Danışmanı: Prof. Dr. Melike NİKBAY

TEMMUZ 2020

Ibrahim Cicek, a M.Sc. student of ITU Graduate School of Science Engineering and Technology, student ID 511171114, successfully defended the thesis entitled “OPTIMIZATION OF DESIGN AND CONTROL PARAMETERS FOR AN ELECTRICALLY-PROPELLED AERIAL VEHICLE USING THE ENERGY APPROACH”, which he prepared after fulfilling the requirements specified in the associated legislations, before the jury whose signatures are below.

Thesis Advisor : **Prof. Dr. Melike NİKBAY** ....
İstanbul Technical University

Jury Members : **Prof. Dr. Ata MUĞAN** ....
Istanbul Technical University

Assoc. Prof. Cüneyt YILMAZ ....
Yildiz Technical University

Date of Submission : 25 June 2020
Date of Defense : 17 July 2020

To my family and friends,

FOREWORD

First of all, I would like to express my gratitude to Prof. Dr. Melike Nikbayfor her guidance and support throughout this study. I am indeed very fortunate to have the opportunity to study at the Faculty of Aeronautics and Astronautics, Istanbul Technical University,under Prof. Dr.Nikbay's precious guidance.

Secondly, I would like to send my gratitude and special thanks to my family for their support in this education period. This achievement has been possible with their encouragement and valuable suggestions.

Lastly, many thanks to my AVL colleagues for their support,encouragement and understanding, I was able to attend the lectures even during someintensive periods of the ongoing projects.

At the Istanbul Technical University Aeronautics and Astronautics Engineering Department, I am also very thankful to the all faculty members for their help during my BSc and MSc education period.

June 2020 Ibrahim CICEK

TABLE OF CONTENTS

Page

ABBREVIATIONS

BEV	: Battery Electric Vehicle
CAGR	: Compound Annual Growth Rate
DC	: Direct Current
EVTOL	: Electrical Vertical Take-Off Landing Aerial Vehicle
HEV	: Hybrid Electric Vehicle
IHSM	: Interval Halving Search Method
IPCC	: Intergovernmental Panel on Climate Change
ISE	: Integral Squared Method
LQR	: Linear Quadratic Regulator
MBSE	: Model-Based System Engineering
MTOW	: Maximum Take-Off Weight
PID	: Proportional Integral Derivative Controller
PL	: Payload, *N*
SE	: Specific Energy, *kW/kg*
SED	: Specific Energy Density, *kW/kg*
SFC	: Specific Fuel Consumption, *g/kN.s*
STOL	: Short Range Take-Off Landing aerial vehicle
UAV	: Unmanned Aerial Vehicle
US	: United States
VTOL	: Vertical Take-Off Landing Aerial Vehicle

SYMBOLS

$\mathbf{A_{sweep}}$	:Sweep volume cross-section area, m^2
AR	: Aspect Ratio
C	: Battery capacity, kWh
$\mathbf{C_{D0}}$	: Parasite drag coefficient at zero angle of attack
$\mathbf{C_d}$	: Drag coefficient,
$\mathbf{C_l}$	:Lift coefficient
$\mathbf{C_{SFC}}$	: Specific fuel consumption coefficient,
D	: Drag, N
E	: Energy, Joule
$\mathbf{E_{battery}}$	: Battery total energy
$\mathbf{E_{climb}}$	: Climbing energy
$\mathbf{E_{cruise}}$	: Cruise energy
$\mathbf{E_{drag}}$	: Drag energy
$\mathbf{E_{kinetic}}$	: Kinetic energy
$\mathbf{F}_{drag}$	: Drag force
F(t)	: System function
$G(\mathrm{t})$	: Global constraint
$G(s)$	: Open-loop transfer function
$H(s)$	: Closed-loop transfer function
I	: Rotational inertia, kg.m^2
$\mathbf{I_{sp}}$	: Specificimpulse related fuel consumption index, N.s/kg
J	: Objective cost function
J*	: Optimum cost
$\mathbf{K_d}$	: Derivative coefficient
$\mathbf{K_e}$	: Back-emf coefficient
$\mathbf{K_i}$	: Integral coefficient
$\mathbf{K_p}$	: Proportional coefficient
$\mathbf{K_t}$	: Motor torque coefficient
$\mathbf{K^i_{min}}$	: Coefficient lower limit at i^{th} iteration

$\mathbf{K^{i}_{max}}$	: Coefficient upper limit at ith iteration
$\mathbf{K^{i}_{opt}}$	: Coefficient lower limit at ith iteration
L	: Lift, N
L	: Inductance, Henry
$\mathbf{M, M_{plane}, M_0}$	: Total mass, kg
$\mathbf{M_a}$	: Non-propulsive airframe mass, kg
$\mathbf{M_b}$	: Battery mass, kg
$\mathbf{M_m}$	: E-motor mass, kg
$\mathbf{M_p}$	: Maximum percentage overshoot, %
$\mathbf{\dot{M}_{air}}$	: Diverted air mass flow rate, kg/sec
R	: Resistance, Ohm
$\mathbf{R^2}$	: Regression value
Q	: Ricatti positive-definite matrix
U	: Voltage, Volt
$\mathbf{U_\infty}$	: Supplied voltage, Volt
V	: Velocity, m/s
$\mathbf{V_{flight}}$	: Flight speed, m/s
$\mathbf{V_{min\text{-}p}}$	: Minimum power required velocity, m/s
$\mathbf{\Delta V_z}$	:Velocity in z-direction, m/s
$\mathbf{W, W_0}$	:Gross weight, N
$\mathbf{W_1}$	:Zero-fuel weight, N
$\mathbf{W_i}$	:Initial weight, N
$\mathbf{W_f}$	:Final weight, N
$\mathbf{W_{fuel}}$	:Final weight, N
W	: Work done, Joule
$\mathbf{P, P_{req}}$	: Power required, kW
S	:Lift surface area, m^2
$\mathbf{T, T_{req}}$	: Required thrust, N
$\mathbf{T_r}$	: Rise time, sec
$\mathbf{T_s}$	: Settling time, sec
$\mathbf{T_p}$	: Peak time, sec
b	: Wing span, m
b	: Friction coefficient, N.m.sec
g	: Gravitational acceleration, m/s^2
h	: Cruising altitude, m

i	: Current, Ampere
$\mathbf{n_{prop}}$	: Propulsive efficiency
s	: Laplace transform sign
t	: Time, sec
$\mathbf{t_e}$	: Flight endurance time, sec
$\mathbf{t_f}$	: Final time, sec
$\mathbf{t_i}$	: Initial time, sec
u(t)	: System input
$\ddot{\mathbf{x}}\mathbf{(t)}$	: System dynamics
x(t)	: System state
x(t)'	: Transpose of x(t) vector
$\mathbf{y_{ss}}$	: System output
$\boldsymbol{\alpha}$	: Angle of attack, rad
θ	: Angular speed, rad/sec
$\boldsymbol{\lambda}$	: Lagrange multiplier
$\boldsymbol{\delta}$	: Damping ratio
ω	: Angular velocity, rad/sec
$\boldsymbol{\omega_n}$	: System natural frequency, rad/sec
e(t)	: Error
e(t)'	: Transpose of e(t)vector
e	:Oswald coefficient/ span efficiency
$\boldsymbol{\rho}$, $\boldsymbol{\rho_{air}}$	: Air density, kg/m^3
$\boldsymbol{\varepsilon}$	: Battery Specific energy, kW/kg

LIST OF TABLES

Page

LIST OF FIGURES

Page

OPTIMIZATION OF DESIGN AND CONTROL PARAMETERS FOR AN ELECTRICALLY-PROPELLED AERIAL VEHICLE USING THE ENERGY APPROACH

SUMMARY

With the recent developments in the aviation industry, the interest in green air transportation has significantly increased over the years. The possibility of green energy sources used in road and rail vehicles could help an alternative option in air transportation as well. After the first development of electrical vehicle concept, Hybrid Electric Vehicles (HEVs) and Battery Electric Vehicles (BEVs) pushed the battery technology to be improved and lead a way to be used for the aerial vehicles as well. The air transport vehicles, considering to be electrified for short-range, regional or urban operations, will depend on energy-based optimization and cost elimination for each flight cycle. The concept of electric aircraft has been studied in recent years because of their innovative appearance and zero carbon emission. Until now, unmanned, vertical or short-range take-off landing, UAV, VTOL/STOL, aerial vehicles are presented for various flight operations. The aerial vehicles powered by electrical energy or driven by e-powertrains are revealed as Electric Airplanes or Electrified Vertical Take-Off Landing Vehicles (e-VTOLs). In this study, the design optimization of the electric air vehicle is presented to develop an approach focusing on the total energy requirement for short-range flights. The developed method is based on the vehicle power consumption for a defined trip/flight profile over a required timespan. Principles of energy requirements during a trip taken into account and the design parameters are estimated. The feasible design proposal is made for short-range flights by suggesting the estimated energy requirement from battery storage. After drawing a rough picture of total energy, the corresponding battery mass, propulsion unit mass, and total vehicle mass is suggested. Since the main energy consumer is the e-motor that generates the propulsion power through powertrain elements, a detail of control parameters optimization is studied for the propulsion unit. In this regard, an online optimization method based on the Optimal Control Theory is proposed for e-motor control parameters. The widely used control method of Proportional-Integral-Derivative (PID) parameters are optimized for the selected e-motor. To come up with the set of optimum PID parameters, the Integral Squared Error (ISE) Method and Interval Halving Search Method (IHSM) are used. All estimations are made with minimum energy requirement consideration. The equations of motions and transfer functions are governed by control and stability equations by introducing the loads exerted on the vehicle. The aerodynamically generated lift and drag, the required e-motor thrust, and total vehicle weight forces during alevel flight are basically implemented.

ELEKTRİKSEL TAHRİKLİ BİR HAVA ARACININ ENERJİ YAKLAŞIMIYLA TASARIM VE KONTROL PARAMETRELERİ OPTİMİZASYONU

ÖZET

Havacılık endüstrisinin gelişmesiyle temiz ve düşük maaliyetli hava taşımacılığına olan ilgi yıllar geçtikçe artmıştır. Özellikle hava veya kara taşımacılığında temiz enerji kaynaklarının önemi, hava araçlarının elektrifikasyonu için alternatif yakıt tüketiminin önemini beraberinde getirir. İlk elektrikli araç konseptinin geliştirilmesinden sonra, Hibrid Elektrikli ve Batarya Elektrikli Araçlar'ın üretilmesi, batarya teknolojisini geliştirmeye ve enerji depolama kapasitesini artırmaya yöneltti. Batarya teknolojisinin geliştirilmesi, hava araçları için de kullanılabilirliği ve hava taşımacılığının yenilenebilir enerji kaynaklarına bağlı olma fırasıtın doğuruyor. Kısa menzilli, bölgesel uçuş operasyonları için elektrikli hale getirilmesi düşünülen hava araçları taşımacılığının verimliliği, her bir uçuş döngüsü için enerji optimizasyonuna ve maliyet eliminasyonuna büyük oranda bağlı olacaktır. Elektrikli uçak kavramı, elektrikli uçakların yenilikçi görünümleri ve sıfır karbon salınımı nedeniyle son yıllarda popüler bir çalışma konusu haline gelmiştir. Şimdiye kadar, dikey veya kısa mesafeli kalkış iniş hava araçları VTOL / STOL, etkili uçuş operasyonları ve hedeflenen manevralara doğrudan ulaşabildikleri için bir çok örneği üzerinde geliştirilmeler yapıldı. Elektrik enerjisi ile çalışan veya elektrik aktarma organları tarafından tahrik edilen hava araçları Elektrikli Uçaklar veya Elektrikli Dikey Kalkış İniş Araçları, e-VTOL'ler olarak adlandırılır. Bu çalışmada, bir hava aracının elektrifikasyonu yapılırken hangi dizayn aralıklarında tasarımın yapılması daha elverişli olacağı, yapılan tasarım için hangi parametrelerin optimize edilmesi gerektiği, optimize edilecek parametrelerin eldesi ve iki farklı tip konvansiyonel uçağın elektrikli hale getirilmesi durumunda menzil ve uçuş tahminleri yapılmıştır. Dikey kalkış-iniş yapacak kısa menzilli hava aracı olan e-VTOL'lerin tasarım parametrelerinin belirlenmesi, kısa mesafeli uçuşlar için toplam enerji gereksinimini göz önüne alarak bir tasarım optimizasyonu ile yapılmıştır. Yöntem, gerekli zaman aralığı boyunca belirli bir yolculuk için araç güç tüketimine dayanır. Belirlenen bir uçuş profili boyunca aracın tüketebileceği toplam enerji ve buna bağlı olarak tasarım parametreleri tahmin edilmektedir. Ayrıca yakıt tankına kıyasla benzer oranda kütleye sahip bir bataryanın kullanılmasının sağlayabileceği toplam ve anlık enerji çıktıları tahmin edilmiştir. Genel dizayn parametreleri elde edildikten sonra itki kaynağı olarak kullanılacak elektrik motorunun kontrol parametrelerinin optimizasyonu için yeni bir yaklaşım sunulmuştur. İtme kaynağı olarak aracın aktarma organında kullanılacak e-motor için kontrol parametreleri, Optimal Kontrol Teorisi'ne dayanarak optimize edilmiştir. Bir dizi optimal PID katsayılarının sunulması için Aralık Yarılama Yöntemi (IHM) geliştirilmiş ve algoritmada kullanılmıştır. Optimizasyon algoritması temel maliyet fonksiyonu göz önüne alarak Optimal Kontroldeki Hataların Karelerinin İntegrali (ISE) Yöntemi benimsenmiştir.

Bütün çıkarımlar minimum enerji tüketimi gereksinimine dayanan objektif fonksiyona göre yapılmıştır. Optimizasyonda kullanılan denklemler ve kontrol sistemin transfer fonksiyonları, araç üzerine uygulanan kuvvet ve yükün, yani aerodinamik kaldırma ve sürükleme, gereken itme kuvveti ve toplam kütle parametrelerinden yola çıkılarak elde edilmiştir.

1. INTRODUCTION

In the late 1800s, Charles Renard and Arthur C. Krebs, military workers and inventors in the French Army Corps of Engineers, built a balloon that was in an elongated shape, called La France airship. La France was experimented with electrically-propelled motors, but they faced problems when the battery run out in a short time due to low capacity [25]. This recurring problem was a big predicament for years. After ten decades, when Nickel-Cadmium batteries were invented, the first flight of an air vehicle with an electric motor was performed. This flight has lasted less than a quarter-hour. The trial of electric flights was not undergone until Lithium-ion batteries were invented in the 1980s. By providing more energy storage density than previous batteries, Li-Ion battery leading innovative planes to be revealed nowadays. Forexample, Solar Impulse 2 got big fame in 2015 since it was fully powered by solar panels and spend 16 months flight for the complete trip around the world. It flew with at an average speed of 45 to 55 km/h as it designed in glider concept with a large aspect ratio. However, Solar Impulse 2 was an innovative movement in the recent decade to emphasize the possibility of alternative energy in the aviation industry. Solar Impulse project inspired many aero-electric studies to go through new designs, especially when authorities started realizing that every time a commercial plane fly, it pollutes the environment, and there is no easy fix. The CO2 emission corresponds to aviation ndustry was about 1 billion tons in 2019, which counts for 2.5% of the global emission [31].

The researchers and commercial companies highlighting that the new era should bring new propulsion methods powered by alternative energy in the aviation industry. Since the electric energy sources from the grid (i.e. solar, wind) are easily accessible and cheap, the air vehicle electrification become a new trend for air mobility as it believed to reduce the burden.

Knowing that many industries have been looking for a transition from fossil energy to renewable sources, alternative solutions in transportation are rapidly evolved over the years. A special report published by The Intergovernmental Panel on Climate

Change (IPCC) in 2018 points out that the current industry gas emissions have an impact of 1.5 °C global warming increase every year. “A Clean Planet for All” named report was published by the European Commission in the response of deep decarbonisation. It highlights the scale of the various sectors’ contributions, including the required transportation level in the EU by 2050. The report emphasizes the severity of the challenge in the need for emission reduction using advanced technologies and fuels in the aviation industry [30].

Transforming from the fuel-based propulsion systems to the zero-emission propulsion system by alternative energy sources and new architectures brings a systematic challenge. The challenges awaiting in the aviation industry for the next decades are to develop and introduce safe, reliable, and affordable up to zero-emission concepts.

To ensure climate-neutral future transportation, transforming aviation towards climate neutrality, will require new designs for propulsion systems such as hybrid, full-electric, fuel-cell design architectures. Such design innovations are expected to lead product development and fleet replacement for the breed of new aircraft with profound targets in performance and efficiency. The Partnership of Clean Aviation illustrates technological progress in aviation clean technology, transition towards climate-neutral targets by proposing new aircraft platforms and configurations in three steps wide-approach. The partnership is aiming to point out the decisive performance steps for new design configurations starting from 2020 progressing for 2030, and 2040 up to 2050 [30].

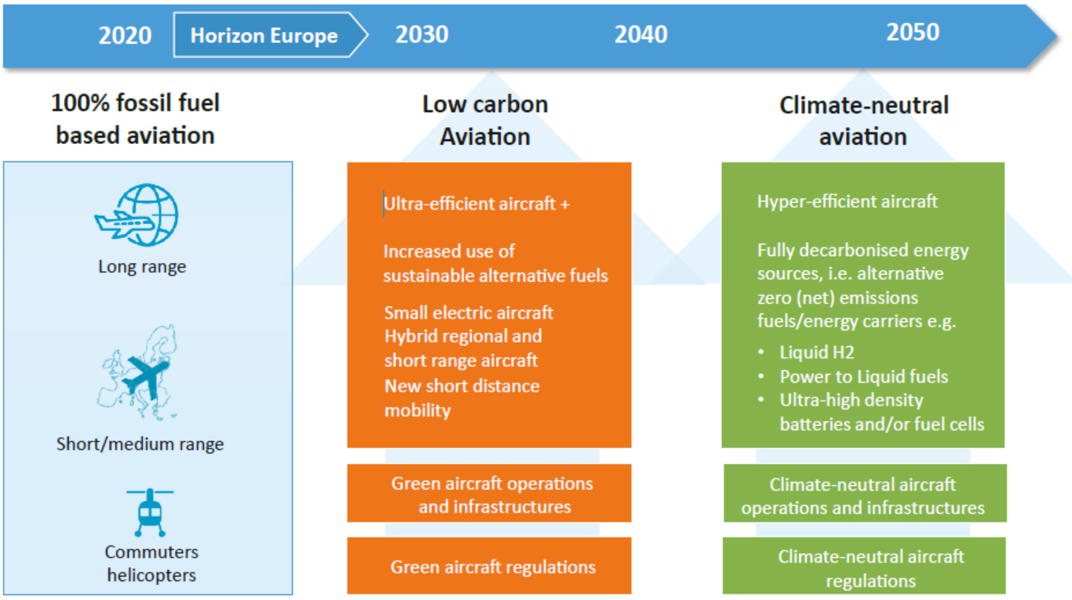

Figure 1.1: Upcoming progress for climate-neutral aviation [30].

Theoretically, some of the carbon-based fuel sources could be replaced by renewable energy sources if we have a reasonable way of producing and storing energy efficiently and effectively. However, the technology required for the aviation industry to use fully-renewable energy is not at a sufficient level. This is due to energy storage limitations during the transport phase (i.e., active flight life cycles). The energy storage dilemma is slowing the adoption of low to zero-emission transportation as the most apparent barrier in the aviation and aerospace industry. For the electrically propelled road vehicles, many companies are producing electric vehicles and solar-powered charging stations since 2008. On the other side, Boeing, Airbus, General Electric, and Rolls Royce are in a continuous challenge to come up with the fuel-efficient planes and powerplants, to enable airliner to save costs. However, they are still using kerosene which charges more than electric energy from the grid that pollutes the atmosphere disregarding climate change regulations. The price of energy used over each flight cycle depicts the demand for low-cost air transportation. Contrary to conventional air transportation, future air mobility is highly expected to have cheap flight tickets, quite airports, and shorter runways.

Similar to every conventional industry being in constant search for the transition to adopting renewable energy, the aviation industry has to overcome the electric energy storage barrier primarily. The energy density of storage methods is limiting the aircraft manufacturers to come up with powertrain electrification for small vehicles. The replacement of a fuel tank by a battery small aircraft class is expected for upcoming years with the help of air mobility encountered by new concepts of VTOLs and STOLs.

The aircraft manufacturers have already promoted the new conceptual designs of cost-efficient next-generation aerial vehicles to optimize the air traffic and flight route networks. Countries that aim to enter the air mobility industry, such as India, Russia, China, and Japan have already started the kick-offs on electrically-propelled aerial vehicles. Several companies have promoted their recent solutions and presented the design concepts at transportion conferences. Since the future promises are challenging for green transportation, the electrically powered vehicles seem to be on a glance, and the feasible designs will be pursued as battery technology can provide [2].

On the similar battery development path, low-cost and light-weight designs are required to have a vehicle flying by using the electric energy for the desired mission. While many new start-up companies have already working on the electrification process, aircraft manufacturers are trying to implement this technology by research & development projects. As the main barrier is the battery cell capacity which can only provide a limited amount of power/energy as it weighs, this phenomenonlead into the weighting limitations. The totalaircraft weightbrings the difficulty of total battery weight to supply propulsion unit over the desired flight range by respecting the constrained battery mass portion. The specifications of old fashioned battery packs are not a sufficient stage to sustain propulsion unit as the petroleum fuels do. Several constraints can be given as an answer to why still two-seated small aircrafts or large transport airliners are not electrified. The first limiting factor is the specific power that the battery can provide during instantaneous discharge without derating. The specific power is the continuous power that vehicle consumes per unit time given in kJ/sec or kW. The second limiting factor is battery energy density which the battery can provide for all operational life cycles after fully charged state, kJ/kg. If we transfer the kJ energy unit to the Watt.hour, the energy density will be represented as the specific energy. In other words, similar to energy density, the main limiting factor is the battery specific energy as it weights per kJ/kg or Wh/kg. Figure 1.2 shows the characteristics of electric batteries with respect to gasoline (jet-fuel). 1

kg jet-fuel (kerosene) can provide 43 MJ energy while Lithium-Ion battery can provide only about 1 MJ [6]. This small amount of energy density of batteries is a highlighted limitation that delaying the electric/ hybrid aircraft development.

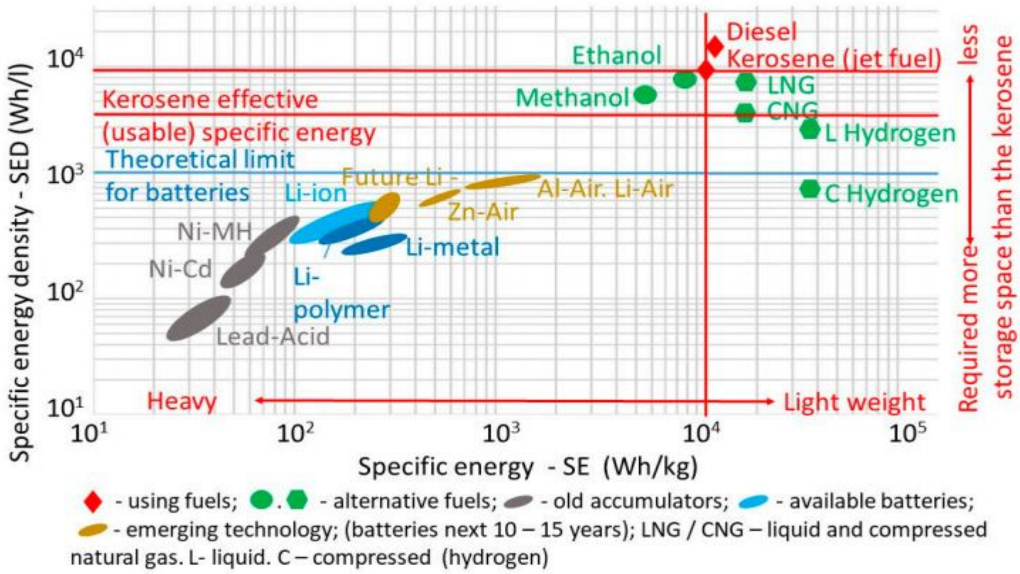

Figure 1.2:Energy density comparison of the applicable fuels [6].

The Lithium-Ion battery can hold an average power of 250 Wh/kg while one small aircraft needs more than 800 Wh/kg to start a take-off flight. This stands quite low in comparison to jet fuel-specific energy, which is about 12 kWh/kg for airliners cruising over long distances. This comparison implies that the design of an aerial vehicle integrated with a battery aiming to provide the same amount of energy quantity requires more battery packs in mass. The greater mass of battery packs requires a higher vehicle weight in total. However, there should be a stage to impose a feasible design criterion. The outcome of the feasibility design range is presented in this thesis that gives us a feasible design range for air transport electrification. With the current battery technology, powertrain electrification is reasonable for short-range flights, especially domestic and in-city operations performed by eVTOLs and small domestic aircrafts.

This thesis presents a design optimization of an aerial vehicle and its motor control parameters by proposing two new methods. It is important to state that the second method is correlated with the first method that specifically narrows down the optimization objective.

The first method is introduced the general electrification process that narrows down the feasibility range for effective aircraft design. Based on current limitations that affect vehicle power consumption, the required optimization for aircraft design is provided. The parameters are defined from aircraft conceptual design and then optimized regarding the power equations. The equations of motion are extracted from aircraft instantaneous power consumption, aircraft dynamics, aerodynamic stability by lift, thrust, maximum take-off weight, and required battery mass. The outcome of the method is given as the maximum accessible range and flight endurance for aircraft class to be electrified.

The second method is about optimizing the control parameters for the propulsion component, which is the e-motor. From the first method, after the determination of the required battery mass and total energy to overcome the desired range, the scope of optimization iszoomed on the e-motor, which is main energy consumer in the powertrain. The dynamic behaviour of e-motor defines the energy consumption profile for a complete mission. Thus, the most critical parameters thought to be optimized in the propulsion unit are the motor control parameters, which are the Proportional Integral Derivative (PID) parameters of the e-motor control system. Based on Optimal Control Theory, the Integral Squared Error Method is used in an online closed-loop system plant. The Interval Halving Searching Method (IHSM)is applied to seek the optimal PID parameters for the objective cost function. In this case, the e-motor control system is considered as a DC motor control system for simplicity. The method provides an online optimal control function can be employed into any control system by improving the transient response. In this case, the employed function reduces the steady-state error for the target motor speed.The thesis briefly structured in four chapters:

Chapter 1 presents the literature review of hybrid/electric aerial vehicles. From a historical perspective, recent studies on hybrid/electric aircrafts are introduced from the global market. The trends on electric vehicles are projected by classifying the vehicles based on their total mass, required power source mass, and operational endurance time.

Chapter 2 introduces the range and endurance calculation of electric aircraft with the help of conventional range and endurance equations to modify design parameters. The method of energy approach is developed to estimate the range and endurance of an electric plane. Calculations are carried out by considering the total energy consumption during the level flight. Required battery mass is extracted from battery specific energy and vehicle power requirement during the entire cruise flight.

In chapter 3, a new method is proposed for any control system optimization. In this case, we aimed to use the new method for integrated e-motor as aircraft propulsion unit. The optimization of motor control parameters is conducted with the help of Optimal Control Theory. DC motor plant model is employed to develop a closed-loop control system with online optimization function used in parallel. The optimization method is a kind of global search optimization by halving the search range of all control parameters simultaneously. To eliminate steady-state error from the closed-loop control process, several constraints are set to obey during all iterations. The objective cost function is equated to Integral Square Error to get as small as possible. DC motor state-space model based on the electric and mechanic equations is derived. A comparison of the closed-loop motor performance is made between the new method and Matlab Tuning function which is without compensation.

Chapter 4 summarizes all significant outcomes by providing the results and suggestions for future works. The calculations are done by aiming at minimum energy consumption of vehicles during level flight. After determining the power requirement from the diverted air approach, the design and control parameters are obtained for better aircraft performance.

1.1 Literature Review

As stated in the introduction section, there will be new types of electric aircraft expected to take place in the market, especially the short-range aircrafts and e-VTOLs. Until now, the Unmanned Aerial Vehicles (UAV) and VTOLS/ STOLS were presented in wide usage. The market of the electrically-propelled aerial vehicles is expected to rise within 10 years by 19.7% [3]. For instance, Rolls Royce aimed to start serial production until late 2020 Spring of ACCEL aircraft integrated with the most power-dense battery packs ever assembled for an aircraft. The Pipistrel company in Slovenia already manufactured and sold 40 Alpha-Electro aircrafts which have been produced for customers across Europe, the US, and Australia and will continue to enhance the number of production. The planes are primarily being used for flying lessons over the airports.

The total market of the electric aircraft was about $498 million in 2019 and is projected to reach $3583 million by 2030 for a total of 500 aircraft, of which would be nearly 10% of private planes [3]. Considering the battery limitations, the expected next-generation electrical aircrafts will have the range up to 500 miles or less. This is also sufficient to fulfill many domestic flights as it will reduce CO2 emission remarkably. A survey of statistics performed by Bussiness Insider shows that the half of all flight tickets sold globally during 2018 were for the flight with a range of less than 500 miles. This is a reasonable evidence to push the electric aerial vehicles in the market for shorter routes. The statistics from MarketAndMarket Research Institutes demonstrate the development and the demand of the e-VTOLs for the next decade [1]. The results from the market research report are summarized by the following highlighted points:

- From 2019 to 2030, the military segment of the VTOL UAV fixed-wing market is expected to rise at the fastest Compound Annual Growth Rate (CAGR) The VTOL UAV market for fixed wings was segmented based on vertical operating mode, range, endurance, propulsion, Maximum Take-Off Weight (MTOW), and wing platform area.
- The UAVs having Maximum Take-Off Weight (MTOW) less than 25kg are expected to have the largest share of the fixed-wing VTOL market in 2019.

- It is projected that the light-weight segment with less than 25 kg will have the biggest share in 2019. It can be due to the huge number of manufacturers selling VTOL UAV products in this segment, as this segment contains a large range of products needed for commercial applications.
- It is expected that the flight endurance more than 10 hours of the VTOL UAV fixed-wing market will have the largest share in 2019

The fixed-wing VTOL UAV industry was segmented in less than 5 hours, 5- hours, and more than 10 hours, based on flight endurance. The segment of more than 10 hours is expected to rise from 2019 to 2030, at the highest CAGR. This rise can be related to the increasing demand for fixed-wing high-endurance VTOLs in military and commercial applications. The following figure represents the geographic distribution of VTOL market projected up to 2030 (Figure 1.3). Table 1.1 represents the current electric hybrid aircrafts with their technical specifications.

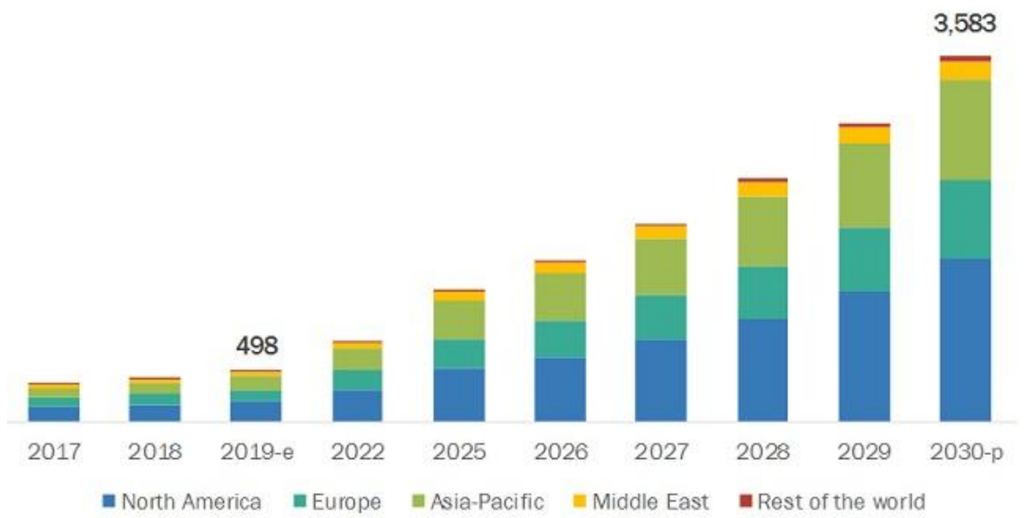

Figure 1.3:Fixed-wing VTOL UAV market by regions in (USD Million) [1].

Table1.1: Technical Specification of some hybrid/ electric Airplanes [32].

	Motor max. Power	**Motor max. Speed**	**Wing Span/Area**	**Rudder/Tail Area**	**Basic Empty Weight / MTOW**	**Propeller diameter**	**Battery Cap./ Voltage**	**Charge type/ charge dur.**	**Range**	**Max. Cruise Speed**	**Flight time**
Pipistrel Aplha-Electro (2seat)	50-60kW (x1)	2100-2400rpm	10.5m / 9.51m^2	1.1m^2 /1.08m^2	368kg/ 550kg	1.8m	21kWh/ 297-300V (130kg)	1 or three phase/ 8 or 1.1hrs	130km	201kph	5-7hrs
Lilium Jet(2seat)	320kW/ 36 (x36)		6m / 2.68m^2	N/A (eVTOL)	400kg/ 600kg	0.15m (x36)	38kWh/ (240kg)		380km	250kph	48min
Alice (2+9 seat)	900-200kW/3 (peak-cruise) (x3)	1900 rpm	16.12 m/		5216kg/ 6350kg		900kWh (3600kg)		1046km	445kph	2.5 hr
Bristell Energic H55 (2seat)	75kW		8.13m/ 10.5m^2		650kg/ 850kg		50kWh (320kg)	1hr		215kph	90min
RR ACCEL	750kW (x3)	2400rpm	7.3m/ 6.5m^2		726/1200kg		/750V (342kg)	2hr / 0.5hr DC	322km	483kph	90min
Zunum Aero ((2+21 seat)	1000kW (Hybrid) (2x500kW e-motor)		15.8m/		4082kg/5216kg(362kg fuel +1043kg batt)		(1043kg)		1126km	547kph	2hr
Bye Aero eFlyer 4 (2seat)	115 hp(90kW)Siemens SP70D		12m/ 12m2		662kg/ 862kg		92-kWh (400kg)			250kph	3.5hr
AE-1 Silent (1 seat)	13 kW (17 hp)		12m/ 10.3 m2		195kg/ 300kg	1.92m	4,1kWh (35 kg)			180kph	
Airbus A³ Vahana (1 seat)			6.25m/		695kg/ 815kg	1.5m			50km	200kph	45min
Boeing PAV	1xH, 8xV electric		8.53m/		575kg/800kg				80km	180kph	

After rearranging the technical specifications in order, the relation between increasing Maximum Take-Off Weight (MTOW) and aircraft Basic Empty Weight (BEW), Payload (PL), and Battery Weight (M_Battery) are plotted in following Figure 1.4, Figure 1.5, and Figure 1.6, respectively. Based on each aircraft numerical data, a trendline curve is also plotted with fitted regression (R2) value in Figure 1.4. After obtaining the regression related to battery weight requirements during operational flight, the next step is to be able to show the feasible design aircraft maximum take-off mass. However, for the new design, the related factors will be implemented to a function to see how the variation of flight endurance changes with aircraft curb weight. The hypothesis of design is defined in the next chapter.

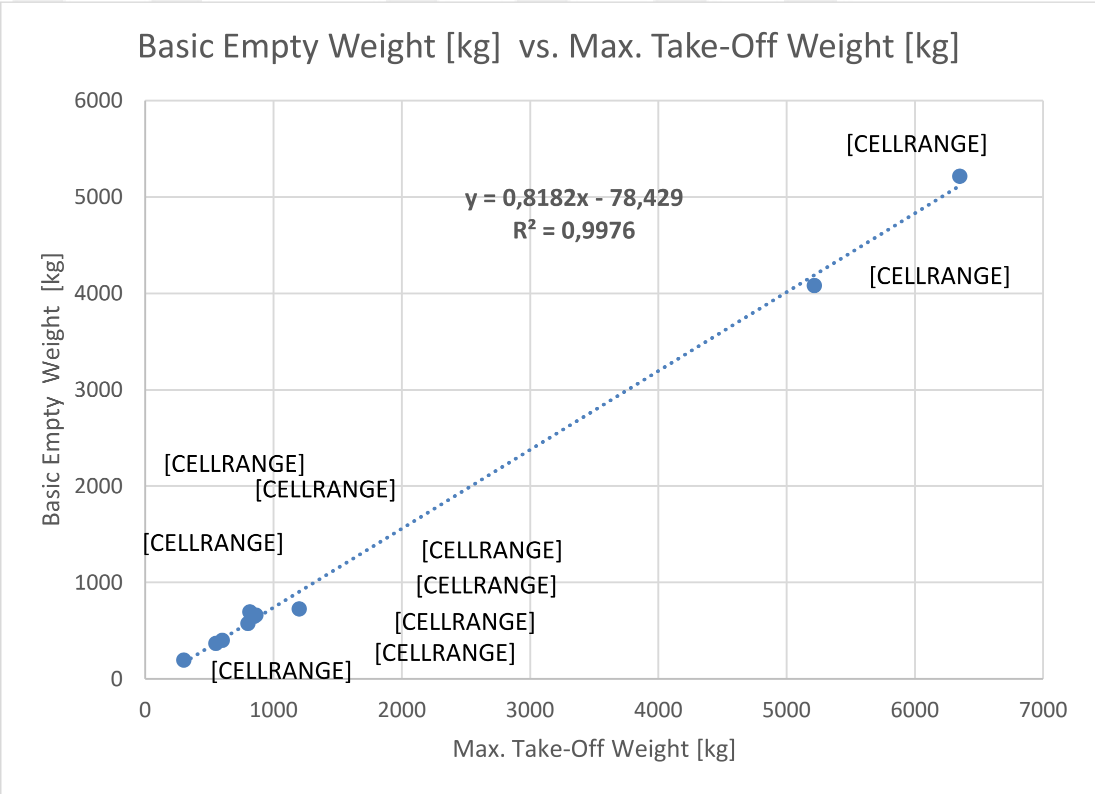

Figure 1.4: The variation of Basic Empty Weight with Max. Take-Off Weight [32].

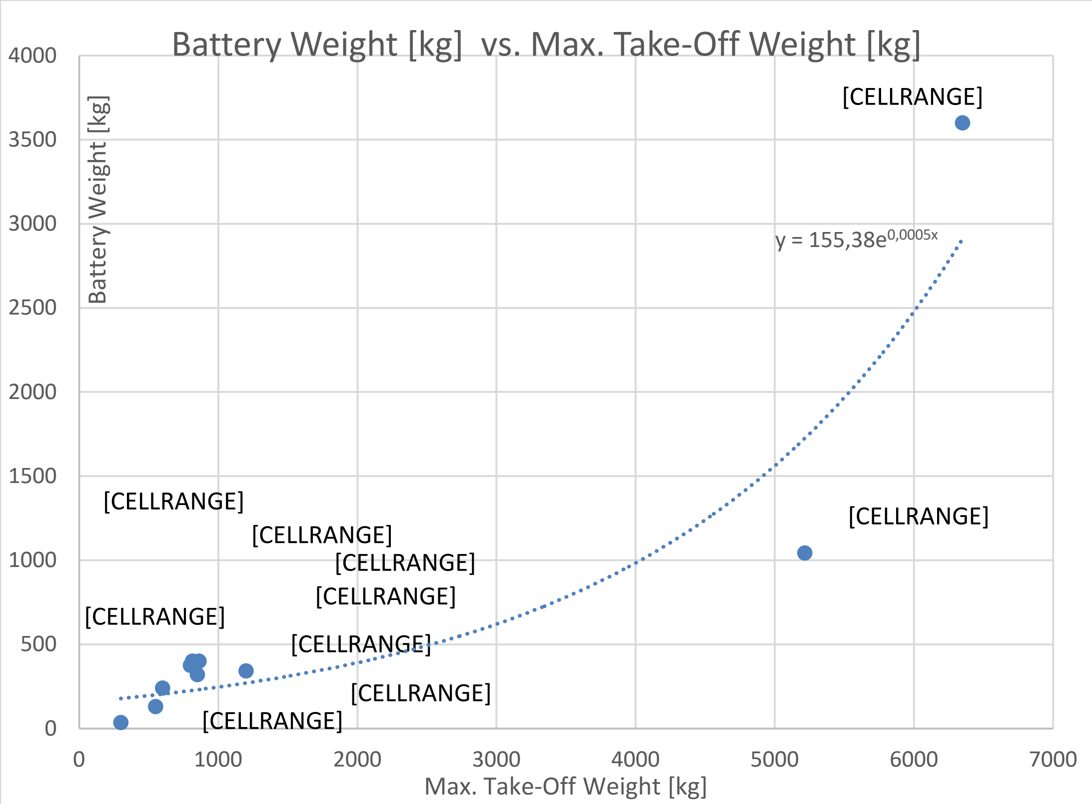

Figure 1.5: Required battery weight as a function ofMax. Take-Off Weight [32]**.**

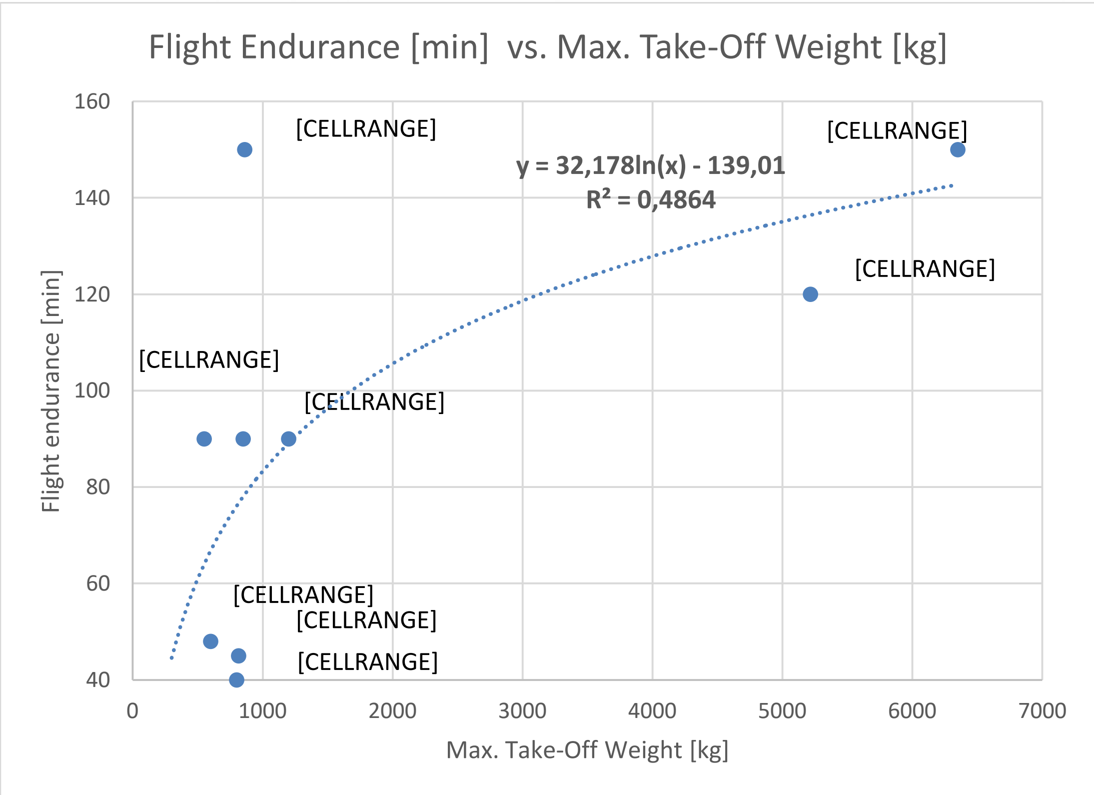

Figure1.6: Flight endurance time variation with Max. Take-Off Weight [32].

2. HYPOTHESIS: SIZING BY CONSUMED ENERGY APPROACH

2.1 Statement of the Problem

Before estimating vehicle sizing, the energy consumed by the vehicle can be expressed in different terminology as energy density (kJ/kg) and specific power (kW). The energy density is a quantity of the energy measure that can be harnessed from 1 kg of a source. The energy density of kerosene that fuel jet airlines use is about 43000 kJ/kg. Currently, even the best Lithium-Ion or Polimer-Ion batteries have energy density around 1000 kJ/kg. This means even the best battery weighs over 40 times than the jet fuel to provide the same energy amount.

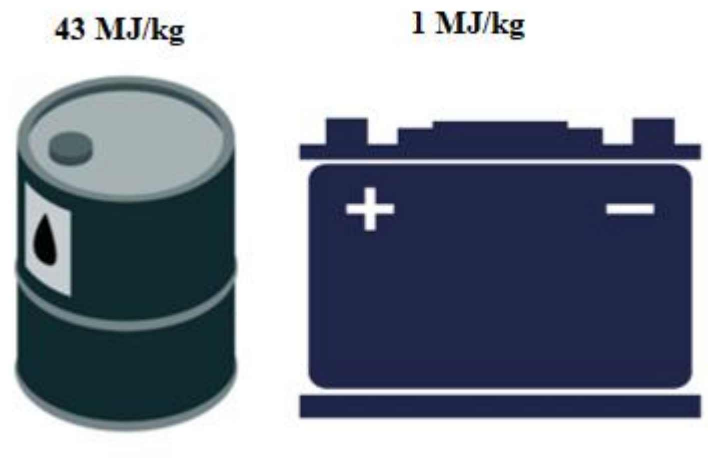

Figure 2.1:Energy density comparison.

These energy density constraints of current battery technologylimits the aerial vehicle electrification as a huge barrier. If we consider a small aircraft for single flight operation in urban cycle powered by battery packs, the trip will have a flight from point A to point B with the following profile.

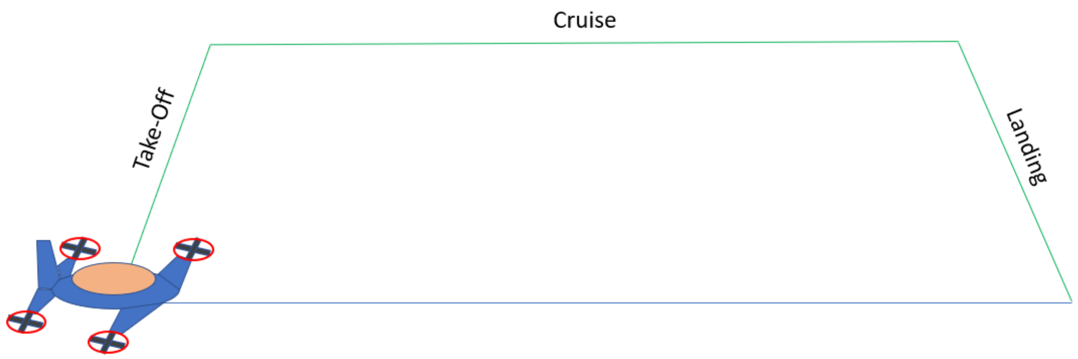

Figure 2.2:Typical flight profile for an aerial vehicle.

To calculate required total energy for this profile the following assumptions are made for simplicity:

1- The energy consumed during take-off and landing phases will cancel each other since the vehicle is elevated at the take-off phase and the potential energy of the vehicle increases relatively. The obtained potential energy is used during landing/gliding phase with or without dramatic thrust.

2- The energy required during a cruise is considered as a function of steady-state battery discharge power, flight duration/endurance and estimated range.

2.2 Mathematical Formulation

For cruising flight phase, we will consider the mechanical energy approach for the amount of required energy. Consider an aircraft weighs M kg Maximum Take-Off Weight (MTO) and needs to fly at a service ceiling of h km. To accelerate the vehicle up to the climb speed of V m/s, we need total energy of mechanical rise&speed up plus drag cover energy;

$$E_{\text{climb}} = E_{\text{kinetic}} + E_{\text{drag}} \quad (2.1)$$

$$E_{\text{climb}} = \tfrac{1}{2}MV^2 + F_{drag}.\int d\,x \quad (2.2)$$

$$E_{\text{climb}} = \tfrac{1}{2}MV^2 + \left(\tfrac{1}{2}\rho V^2.\mathrm{S}.C_d\right).\Delta x \quad (2.3)$$

For the level flight, the aircraft has to overcome total lift plus total drag force over a range of distance for a flight duration at a constant cruise speed *V*. The total energy required for this phase is a function of total thrust which is required to move the aircraft at cruise speed and overcome the total drag force (parasite + induced drag):

$$\frac{dE_{cruise}}{dt} = \left(\tfrac{1}{2}\rho V^2.S.C_l + \tfrac{1}{2}\rho V^2.S.C_d\right)dx \quad (2.4)$$

$$E_{\text{cruise}} = \int_0^{t_f}\int_0^{x_f}\left(\tfrac{1}{2}\rho V^2.\mathrm{S}.C_l + \tfrac{1}{2}\rho V^2.\mathrm{S}.C_d\right)dx.dt \quad (2.5)$$

Considering a plane cruising at a defined altitude, when lift equals the weight, the power required for forward movement defined as thefunction of total mass, flight speed, plane cross-sectional area and air density. More power requires more battery cells to sustain continuous power demand of the propulsion system. To come with understandable reasoning, two aeroplanes will be compared for electrification to demonstrate if that is possible at least for this moment. The subjected aircrafts are transport airliners such as A320 and small private aircrafts like CESSNA. In this case, we are interested in knowing the power requirements for the flight and the total energy supply that battery shall provide. We will employ the “Work-Energy Theorem” by Formula 2.6.

If a point mass, weighted m kg moved in the direction of applied force F N for x meters (Figure 2.3), the work done is W Jouleandit is formulated by work-energy theoremas follows:

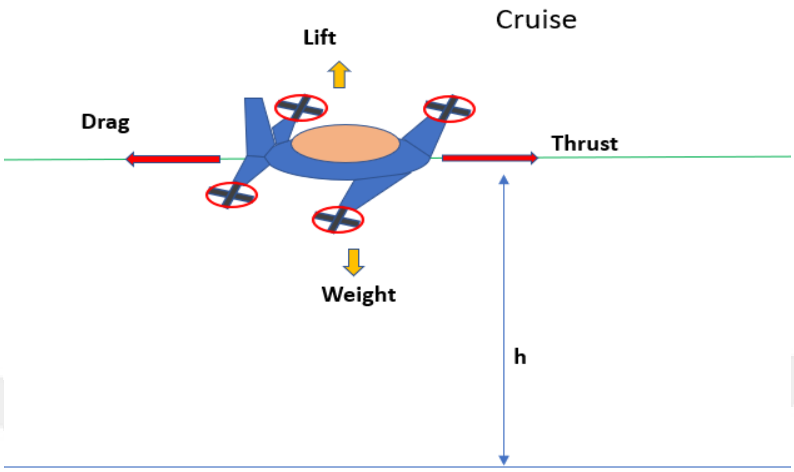

Figure 2.3:Aircraft cruising at h altitude.

$$W = \int_{x=0}^{x=x_f} F.dx. \tag{2.6}$$

Then the power is the rate of work done, energy consumed per unit time

$$P = \frac{dW}{dt} \tag{2.7}$$

We get an equation for power that equals force multiplied by distance divided by time:

$$P = F.\frac{\Delta x}{\Delta t} \tag{2.8}$$

$$P = F.\Delta V \tag{2.9}$$

Now the propulsion system requirement is to maintain a steady level flight since the thrust must be equal to the drag;

$$T_{req} = \mathrm{D} \tag{2.10}$$

$$P_{req} = T_{req}.V = D.V \tag{2.11}$$

$$P_{req} = \frac{1}{2}\rho V^3.S.C_{D0} + \frac{W^2}{\frac{1}{2}\rho VS}\left(\frac{1}{\pi eAR}\right) \tag{2.12}$$

Thus the power requirement of an aircraft (for steady level flight) will have the form illustrated in Figure2.4.

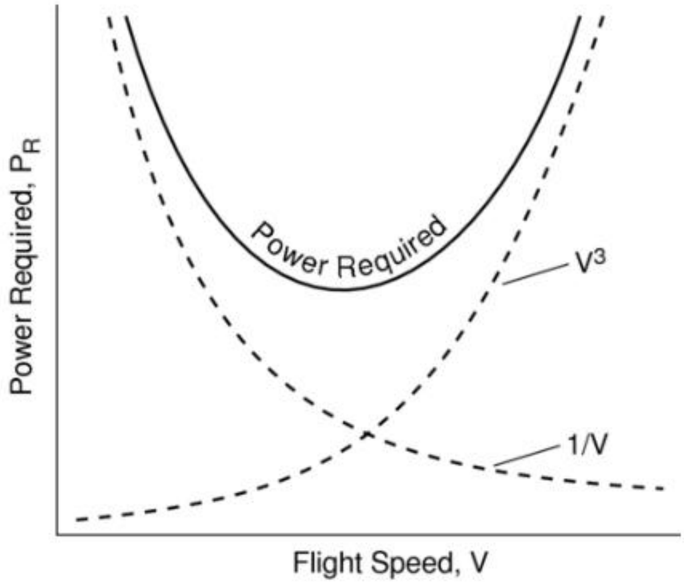

Figure 2.4: Level flight power required curve for an aircraft [4].

By taking the derivative of the equation for the required power, P_{req}, concerning $V$and setting it equal to zero, the velocity for minimum power is obtainedas follows:

$$V_{minimum} = \left[\frac{4}{3}\left(\frac{w}{S}\right)^2 \frac{1}{\rho^2 C_{D0}}\left(\frac{1}{\pi e AR}\right)\right]^{\frac{1}{4}} \quad (2.13)$$

The maximum endurance (flight time) is obtained and this implies that minimum power is used to maintain the steady level flight (i.e., minimum continuous energy discharge from the battery). Maximum range (distance travelled) is obtained for the aircraft with the most aerodynamically most efficient condition (at maximumC_L/C_D).

In this case, the minimum required velocity is the velocity optimized for overcoming to the parasite drag and induced drags (i.e. proportional with V^3 and V^{-1} respectively). The airstream is relatively diverted by downstream of the airplane so we assume that the optimum velocity is equal to downstream velocity in the downward direction of z. ($\Delta V_z = V_{minimum}$). This is the downward velocity of the air that the plane diverts it downward. Since the direction is downwards, we denote this velocity as ΔVz. The value of the downward velocity is obtained from the aerodynamic lift equation. The powering force of the movement is the thrust force-generating sufficient lift that holds plane against its weight. Based on the balanced force that lift equals the weight, the lift is substituted in power equation as follows:

$$P = M_{plane} \cdot g . \Delta V_z \tag{2.14}$$

Here, the total aircraft mass, M_{plane} , is considered as the maximum take-off mass, M_{MTO}. It is the summation of payload mass M_p, non-propulsive airframe mass M_a, electric motor mass M_m, and battery mass M_b. At this point, the non-propulsive airframe mass (structure, on-board system, landing gear etc.) is given for all airframe except the powertrain components (e-motor+inverter, battery).

$$M_{MTO} = M_p + M_a + M_m + M_b \tag{2.15}$$

The mass and power estimation procedure strongly determines the reliable airframe sizing, and it inherently depends on motor thrust and wing surface. Total energy demands determine the battery sizing and motor power consumption for the specified mission requirements. Then, power and wing surface are determined by choosing the design point in the feasible design space drawn based on Thrust-to-Weight ratio (T/W) and Wing-Loading (W/ S), which takes all points and performance requirements into account [8]. In this manner, aircraft mass, engine thrust and wing surface can be dimensioned and correlated with power requirement.

The lift of an aircraft must be equal to the delivered downward momentum rate to the air it displaces. This means that the total weight must be equal in magnitude to the downward velocity of the deflected air, times the rate of deflected air:

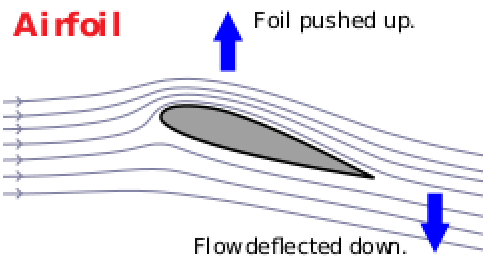

Figure 2.5: Typical airfoil.

Based on the Kutta's lift theorem generated by air circulation, the generated lift is equal to mass flow rate diverted downward direction and shall be equal to plane weight during steady flight [10].

$$W = L \qquad\qquad M_{plane} \cdot g = \dot{M}_{air} \Delta V_z \tag{2.16}$$

The total mass of the air that exerted on the plane is simply the volume of the enclosed air that it sweeps out per unit time, multiplied by air density. The enclosed air is assumed to be circular shaped by tip vortices that induced drag generates. If we denote the relevant cross-sectional area, A_{sweep}, then the volume it sweeps out per unit time is volumetric airflow. Therefore, the mass flow rate equals the density of air times the cross-sectional area times the velocity of air:

$$\dot{M}_{air} = \rho_{air} \cdot A_{sweep} \cdot V_{flight} \tag{2.17}$$

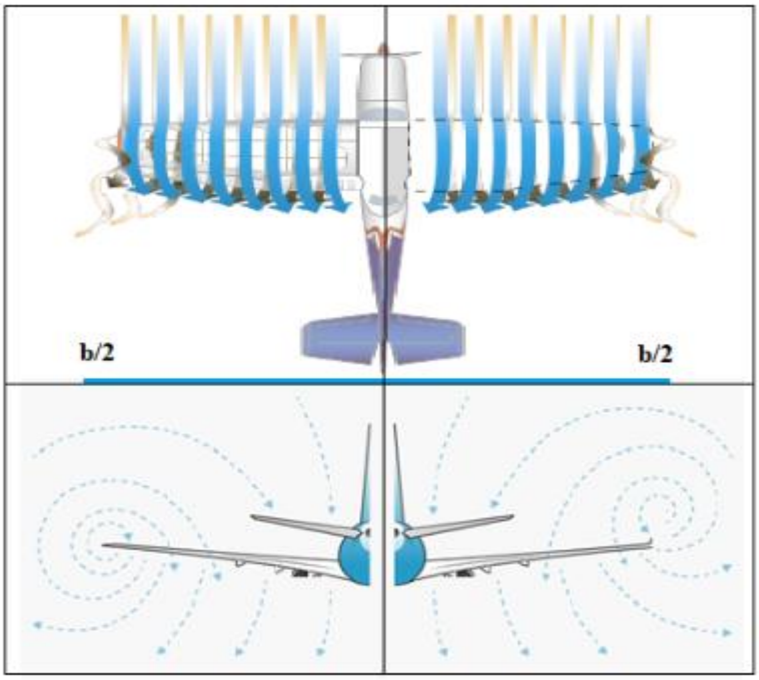

Figure 2.6: Swepped air during flight.

Now the only unknown parameter is A_{sweep}, which is the projected cross-section area of the projected aircraft including air influences in its surrounding. This area depends on the relative aircraft velocity and the surrounding air at the cruising condition. The vortices that plane dissipates have roughly the radius of the length of the plane's wings. Approximation to this relevant area becomes the total length of the wing length$b$. Then, we can assume the total cross-sectional area become a circular area of the swept air.

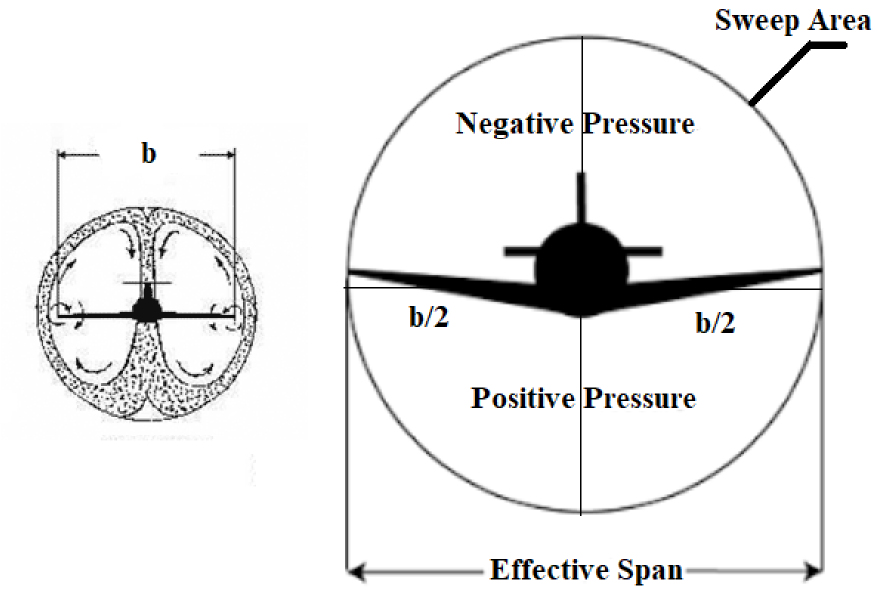

Figure 2.7: Circularly assumed swept air.

$$A_{sweep} = \pi \frac{b^2}{4} \quad (2.18)$$

$$F_{flight} = \dot{M}_{air} g = \Delta V_z \, \rho_{air} A_{sweep} V_{flight} \quad (2.19)$$

$$\dot{M}_{air} . g = \Delta V_z \, \rho_{air} A_{sweep} V_{flight} \quad (2.20)$$

$$\Delta V_z = \frac{M_{plane} \, g}{\rho_{air} A_{sweep} V_{flight}} \quad (2.21)$$

$$P = M_{plane} g \, \Delta V_z \quad (2.22)$$

Getting all terms together, the liftforceof the aircraft needs to provide adequate power to overcome the consumption coming from swept air. This equation boldly emphasizes that the plane is sweeping out a tube of air and shifting it downwards.By this downward acceleration of air,it becomes equal to the downward pull of the plane weight. So the aircraft propulsion system avoids falling by constantly paying the power of streaming momentum downward via the sweep air. Rearranging Equation2.19, Equation2.20 and Equation2.21 to solve for ΔV_z in terms of quantities,the instantaneous power can be easily measured. And plugging it into Equation2.22, the overall power required for lift is given in the form below:

$$P = \frac{4.{M_{plane}}^2 .g^2}{\rho_{air} .\pi b^2.V_{flight}} \tag{2.23}$$

This equation importantly depicts that the variables affect the energy requirements of the plane.

Remarks: As the aircraftflies at a higher velocity the power required for the propulsiondecreases, but the effect of the parasite drag is negligible in Equation 2.23. The total power required to fly at cruising level is minimized when the lift and drag are equal (motor thrust = drag force). Since the propulsion systemconsumes energy for both diverting the sweptair, generating lift forceand overcomingthe parasite drag as it equals to thrust, the equation can be simply doubled to get total power requirements at cruising speed. Then it becomes:

$$P = \frac{8.{M_{plane}}^2 .g^2}{\rho_{air} .\pi b^2.V_{flight}} \tag{2.24}$$

- Now, it is obvious why increasing the aircraft maximum take-off mass is such a huge issue for electric flights. The mass component of the power equation is squared and doubled as well. Doubling the total aircraft mass will require the power requirements by 8 times.
- The instantaneous power required to move aircraft forward strongly depends on cruise speed, total mass and wing-span.

2.3 Comparison of Existing Aircrafts

By the help of outcomes from the previous section, a calculation is performed for the real-world consequences of comparing an airliner (A320) and small jet aircraft CESSNA. Initially, the battery weight is assumed asthe usual fuel mass fraction. This fraction is considered about 20% of the aircraft total mass. The effect of altitude on air density at the cruising condition shall be considered such that it is less than at sea level. For the CESSNA cruising altitude, the density is divided by factor of 2 (ceiling altitude) while density at the A320 cruising altitude decreased by a factor of 3 (ceiling altitude). Now, we will use the Equation (2.23) to estimate power demand for each aircraft with the following specifications given in Table 2.1.

Table2.1: Technical Specification of compared two aircraft [33, 34].

Spesifications	CESSNA	Airbus A320
Wing Span, b [m]	11	35.8
B.Empty Weight [kg]	736	22700
Payload [kg]	376	19900
M_{TOW} [kg]	1113	78000
Fuel Capacity [US gal]	52-66	24200 – 27200
Weight-to-Thrust	9.25 kg/kW	6.878
Cruise speed, Vcruise [kph]	228 (63.33m/s)	871 (242m/s)
Max. service alt., h [m]	4116	12500
ρ_{air} @service altitude, $\rho_{air} = \rho_{sl}(1 - h/45442)^{4.256}$	0.817 kg/m^3	0.254 kg/m^3

$$P_{CESSNA} = \frac{4(1113kg)^2(9.81ms^{-2})^2}{(0.817kgm^{-3})\,\pi(11m)^2(63.33ms^{-1})} = 243\ kWatt$$

$$P_{A320} = \frac{4(78000kg)^2(9.81ms^{-2})^2}{(0.254kgm^{-3})\pi(35.8m)^2\,(242ms^{-1})} = 9462\ kWatt$$

Considering the specific power of Lithium-Ion battery which is about 0.35kW/kg. To supply the electric planes power demand, A320 needs27000kg of the battery pack (9462kW/0.35kW.kg-1) assumed that the fuel amount is to be 22700kg in the tank before starting the flight. Similarly,CESSNA would need just 694kg (243kW/0.35kW.kg-1) with approximately 750kg of fuel to be in the tank.The power requirements are almost fulfilled for both aircraft considering the negligible efficiency losses. However,we need to keep in mind that this is just the instantaneous power that eachaircraft requires at any cruise flight instant. The main goal is to obtain the total battery weight requirementfor thedesiredflight time.

To demonstrate how the electrified aircraft to have a mass portion, the batteries are replaced with the fuel tank, the obtainable range and flight endurance are re-calculated. For the battery replacement with the fuel tank filled by Jet-A which has a specific energy of 11950Wh/kg, CESSNAelectrification is more favourable than A320, considering the totalfuel weight.If the best storable capacity of Lithium-ion battery could be used, the amount of energy stored would be about 280 Wh/kg. The replacement of 750kg Jet A fuel with Li-Ion Battery will require 7800 kg of a battery pack for CESSNA, which is almost 10 times itsempty weight. For A320 battery replacement, considering the 22700kg Jet-A fuel in its tank, the required battery weight to supply the total energy is around 675000kg.It countsalmost 30 times of the aircraft basicempty weight. The power - energy formula tell us that the required total energy for a flight operation is given by the instantaneous power times flight duration:

$$E_{battery} = P_{flight}.t_f \tag{2.25}$$

Rough assumption can bedonenot to reduceflight speed or increase the total energy used in the same flight. The question is to see how much the total range decreases forsimilar cruise speed and required total energy.As mentioned above, the flight endurance forCESSNA’s flight decrease from 4 hours to about 2 hours. Considering two seated CESSNAthatneeds about 150kg fuel and 200kg payload,the outcome of this calculation depicts the electrification of CESSNA with the required battery capacity decreasing the payload, lowering the cruise speed, increasing wingspan, with lighter structure and efficient electric motors, will be adequate to have a trip of 2 hours flight.This is the actual proof of small electric aircraft coming into the market for recent years such as Pipistrel Alpha Electro, CriCri, Solar Impulse. However, the electrification of A320 is substantially inefficient since it decreases the flight endurance from 7hrs to just 20 minutes.

In Figure 2.5, the relation of flight time/ endurance is shown as a function of mounted battery for both aircraft classes CESSNA and A320.

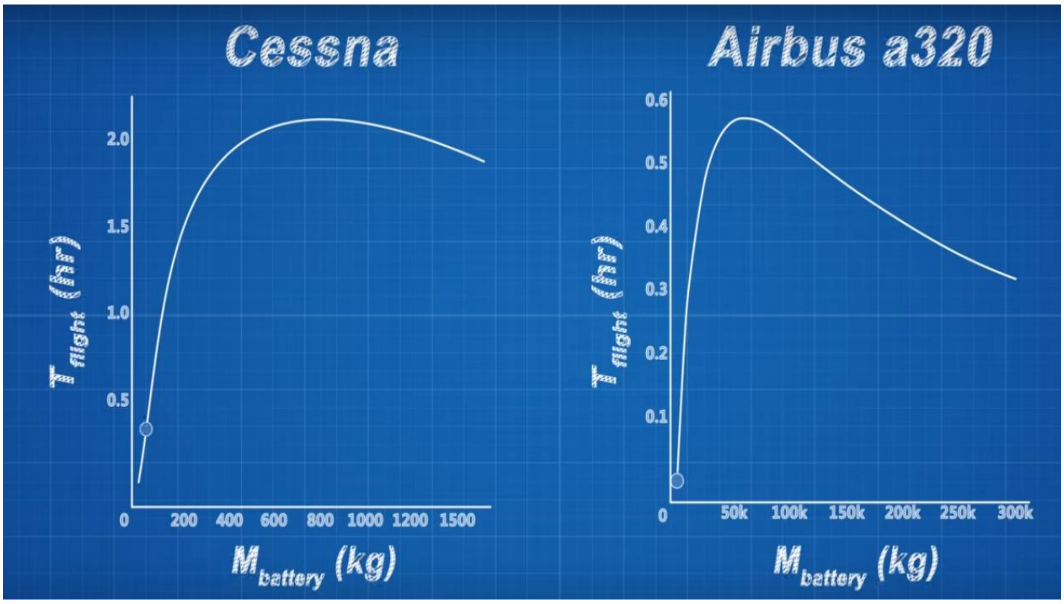

Figure 2.8:Flight time variation as a function of replaced battery weight [31].

2.4 Hypothesis Outcome: Range and Endurance Calculation

2.4.1 Conventional range and endurance calculation

Once the optimal range of battery mass determined, the initial sizing process will be defined for the feasible aircraft design parameters. The design parameters are calculated by considering the Wing-Loading (W/S) and Thrust-to-Weight ratio (T/W). In this manner aircraft mass, enginethrust and maximum take-off mass can be determined in accordance with the configuration decisions [8]. At this point, while determining the aircraft range and endurance, the Breguet equation which is applicable for conventional aircraft shall not be used since the weight ratio term violates the equations as shown below [27]. The logarithmic term will be equal to 0 since weight fraction remains constant during the entire flight regime for electric aircraft (i.e. initial weight,W_i, to final weight, W_f, will remain constant).

$$Range = V_{flight}.t_f = V \cdot \left(\frac{L}{D}\right) \cdot I_{sp} \cdot ln\left(\frac{W_i}{W_f}\right) \quad (2.26)$$

In another form:

$$Range = V_{flight}.t_f = \frac{V_{flight}}{g} \cdot \frac{1}{SFC}.\left(\frac{L}{D}\right) \cdot ln\left(\frac{W_i}{W_f}\right) (2.27)$$

Here, the range is considered as average flight speed, V_f, multiplied by flight time, t_f. The lift-to-drag ratio, L/D is aircraft designer geometrical parameter, while I_{sp} indicates the propulsion system designer based on specific fuel consumption, SFC.

Anderson and Payne governed a manipulated Breguet equation considering the maximum endurance during loiter time as follows:

$$t_{end} = \frac{n_{prop}}{c_{SFC}} \cdot \sqrt{2\rho_\infty \mathrm{S}}.\left(\frac{C_L^{\frac{3}{2}}}{C_D}\right).\left(\frac{L}{D}\right) \cdot \left(\frac{1}{\sqrt{W_1}} - \frac{1}{\sqrt{W_0}}\right) (2.28)$$

Where t_{end} is the endurance time. Similar to the range equation, the Anderson and Payne equation accounts for fuel burn during loiter, assuming the maximum operation at $[C_L^{\frac{3}{2}}/C_D]_{max}$ to enhance endurance performance. The outcomes from range and endurance equations to enhanceperformance can be given as the following conditions:

- Minimize fuel consumption, C_{SFC} or SFC
- Maximize the propeller efficiency, n_{prop}
- Maximize the gross weight to zero fuel weight ratio, W_0/W_1.

  where $W_0 = W_1 + W_{fuel}$
- Maximize the aerodynamic condition $[C_L^{\frac{3}{2}}/C_D]_{max}$
- Flight at maximum air density condition, ρ_∞ which is at sea level.
- Maximize the lifting surface, S, as a summation of wing+tail+body…
- Maximize lift-to-drag ratio, L/D, by choosing proper airfoil and design shape.
- Subject the flight to maximum air density condition, ρ_∞ which is at sealevel.

2.4.2 Electrical range and endurance calculation

For the battery-powered electric aircraft, the total weight of aircraft remains constant during all flight regimes. This is because the battery pack provides constant electrical energy from chemical reactions through Galvanic cells, as there is no fuel to burn. Hence, the range of aircraft is defined as equivalent to the flight speed multiplied by flight time:

$$Range = V_{flight}.t_f \tag{2.29}$$

The range is defined based on battery performance instead of the suggestion by Payne equation. The battery capacity, E_{bat}, average drained current (i_∞) and supplied voltage (U_∞) are the parameters used for range/endurance calculations. The battery capacity can also be represented as the product of the battery mass (M_{bat}) and battery specific energy (ε) [27]. As a result, the maximum endurance (t_{end})is obtained at acondition which corresponds to the minimum power required velocity (V_{min-p}). The flight endurance in a unit of time is calculated as a function of battery mass, battery specific energy and drain power (P_{drain}).

$$t_{end} = \frac{E_{bat}}{i_\infty.U_\infty} = \frac{M_{bat}.\varepsilon}{P_{drain}} \tag{2.30}$$

Substitution of flight time in range equation, we get:

$$Range = V_{flight}.\frac{M_{bat}.\varepsilon}{P_{drain}} \tag{2.31}$$

Also, we need to state that the power drained from the battery is the amount of power that the aircraft requires during the instantaneous flight ($P_{drain} = P_{aircraft}/n_{total}$). Here, the $P_{aircraft}$is the power /obtained in Chapter 1, whichis aircraft consumes through swept area and the n_{total} is the overall propulsion system efficiency. Thus, the power required for aircraft depends on *L/D* ratio and flight speed. Then we get:

$$P_{drain} = \frac{M_0.g}{\left(\frac{L}{D}\right).n_{total}}.V_{flight} \tag{2.32}$$

If we substitute Eq 2.32into Eq 2.33, we will get the overall range of battery-powered aircraft as the form:

$$Range = \frac{M_{bat}.\varepsilon.\left(\frac{L}{D}\right).n_{total}}{M_0.g.V_{flight}} \tag{2.33}$$

To simplify the range equation:

$$Range = \varepsilon.n_{total}.\left(\frac{1}{g}\right).\left(\frac{L}{D}\right).\left(\frac{M_{bat}}{M_0}\right) \tag{2.34}$$

Similar to the Breguet and Payne equations, the range significantly depends on;

- Maximum battery energy density, ε
- Maximum battery mass-to-total aircraft mass ratio, M_{bat}/M_0
- Maximum propulsion system efficiency, n_{total}
- Maximum lift-to-drag ratio, L/D

3. OPTIMIZATION OF CONTROL PARAMETERS BY INTEGRAL SQUARED ERROR (ISE) METHOD

3.1 Introduction

Electrically propelled vehicles, either road or aerial vehicles are recently studied for their robust maneuvers and cost-efficient transport operations. The main power generating systems of such vehicles electrified by selecting the proper components and assembled as e-powertrain. Generally, e-powertrain components are selected by considering the target performance requirements. Since the main component of propulsion is the drive unit, the e-motor control system is subjected to achieve the performance targets. In this chapter, the optimization of e-motor control parameters studied by Integral Squared Error Method (ISE). The overall aim is to minimize the power consumption of such vehicles depending on mission profile and maintaining smooth manoeuvres for passenger comfort. The sought-after values of control parameters are computed using the Optimal Control Theory. The system is modelled as a closed-loop linear control system with calibratable parameters. The objective is to optimize e-motor control system parameters using a comprehensive online search method for each desired input. The goal is to minimize objective cost function by eliminating the steady-state error of the system. For each search iteration, the range of feasible parameters isobtained in the response of sequential inputs while keeping the pre-defined constraints. The system architecture is represented by Model-Based Systems Engineering (MBSE) approach. Deploying the online optimization for control parameters, the system outputs feedback to the model by narrowing down search interval. The model includes the online optimization algorithm to minimize the objective cost function, which is in parallel calculation implemented in model observer and error inputs to offer new parameter trials. In this case, the employed performance constraints parameters are rise time, settling time and percentage overshoot of the system states over a specified time interval. These parameters are the inputs as well for performance measurement function which is punished by integrated square.

3.2 Problem Definition

The optimization problem is modelled by a mathematical representation of optimization variables with integral squared error measure J. The optimal control problem is described by introducing the system dynamics $\ddot{x}(t)$ depending on system input u(t). To consider constraint, Lagrange multiplier coefficient λ is included to re-formulate the following objective function;

Minimize the overall function of:

$$F(\ddot{x}, u, t) \quad (3.1)$$

Subject to the global constraint:

$$G(x, t) \quad (3.2)$$

Then it becomes to minimize the Lagrange combined function:

$$J = F(\ddot{x}, u, t) + \lambda G(x, t) \quad (3.3)$$

Parameters related to the performance measure are maximum percentage overshoot, rise time and settling time. The graphical definition of each performance measure parameters isshown on the figure.

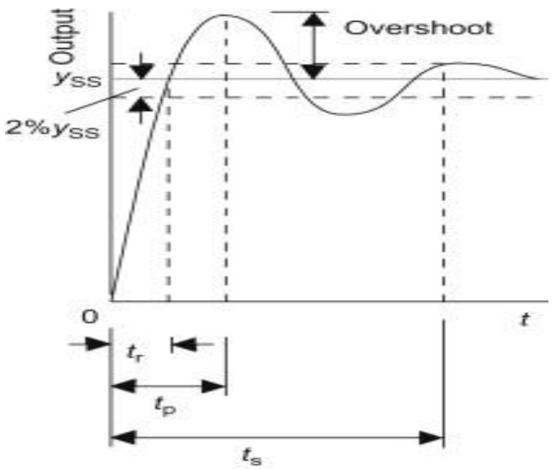

Figure 3.1: Standard damped closed-looposcillatory system (Science Direct).

Here,based on the system input *x(t)*the overshoot is denoted as M_p, the steady-state value is shown as y_{ss}, the rise time, peak time and settling time are defined asT_r, T_p, T_srespectively.The graph is corresponding to a damped oscillatory system with an undamped natural frequency ω_n and damping ratio δ.

The maximum percentage overshootM_p is generally written as a percentage of the steady-state value.Graphically represented as the amplitude of the first peak, it is the maximum valueat which the response exceeds the steady-state amount.

$$M_p = 100\, e^{\frac{\pi\delta}{\sqrt{1-\delta^2}}} \tag{3.4}$$

The rise time T_r is the time for the response of the system taken from 0 to 90% of the steady-state value.T_r is the time to complete the quarter (i.e. ½π) of the oscillating response.

$$T_r = \frac{1}{\omega_n}(2.3\delta^2 - 0.078\delta + 1.12) \tag{3.5}$$

The settling time T_s is the time taken for the system response to settle down near steady-state value by a specified percentage (typically 10% of deviation).

$$T_s = -\frac{ln\,(tolerance)}{\delta\omega_n} \tag{3.6}$$

The control system ofe-motor is modelled andrepresented as a closed-loop system with unit step input for simplicity. The calculation performed by running the optimization module parallel with the loop is done within the time interval of [t_i=0, t_f]. Heret_i is the initial time when systems start andt_f is the arbitrary final time.

After rearranging the online optimization and controller module, it is aimed to be mounted in Electric/Hybrid powertrains. The system architecture is designed by Model-Based Systems Engineering (MBSE) approach. The closed-loop control system with parallel optimization approach is shown below.

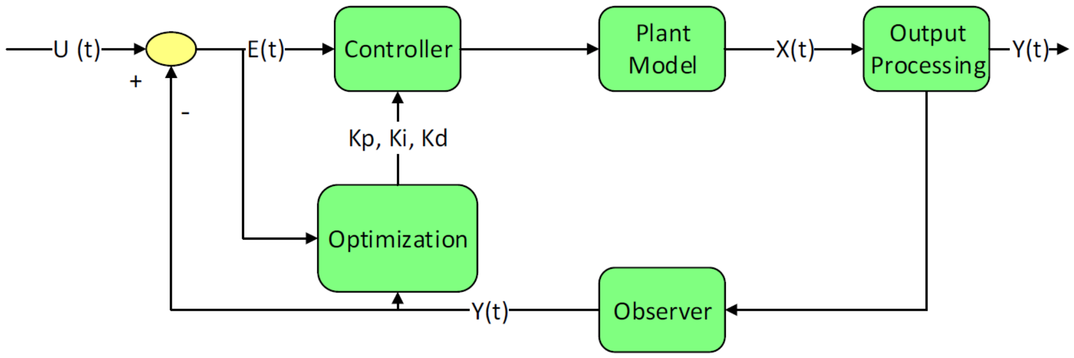

Figure 3.2: Closed-loop control system.

3.3 Interval Halving Search Optimization

The Interval Halving Search Method is the method that is searching the optimal point by dividing the previous searching range by factor of 2. This method is grantedwith improved search resolution by ascending increment. After each step of division, the range of search is halved and resolution improved ten times than the previous step. In this study, the resolution increment is set to 0.1 at the initial step. For each subsequent step, the resolution improved10 times after halving interval range by dividing search range to 10. The aim is to seek the target optimal points more precisely with small searching increment [34]. In Figure 3.3, available all Search Optimization methods are given in chart by classified hierarchy.

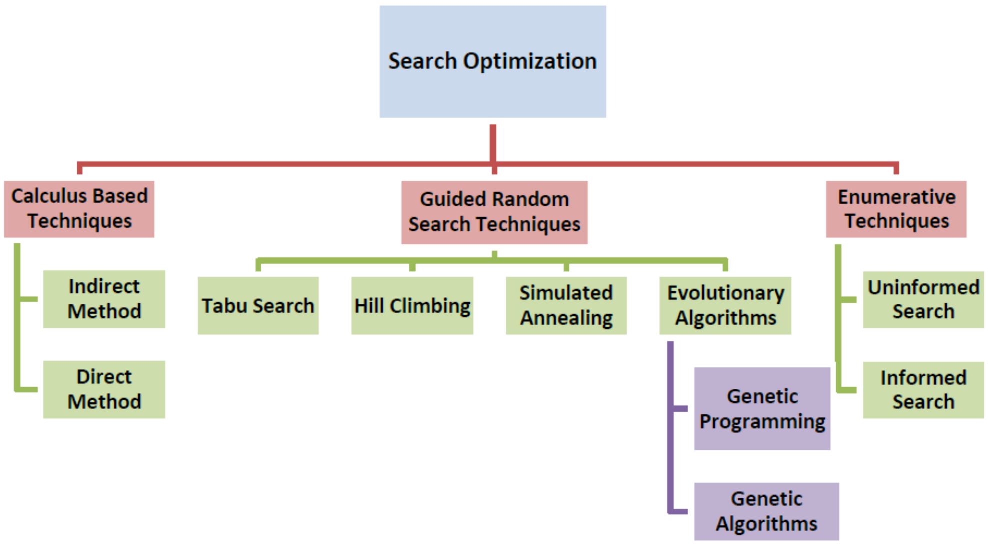

Figure 3.3: Search Optimization methods currently in use.

The Interval Halving Search Method is mathematically formulated which can be seen in Figure 3.4. Starting at lower to upper defined limits at first step (K1min, K1max) for each parameter, the set of first feasible values are assigned to the $K^1_{P\_opt}$, $K^1_{I\_opt}$ and $K^1_{D\_opt}$. Then the search range is narrowed down for the next step by shifting the lower limit to

$$K^2{}_{P,I,D\_min} = \frac{(K^1{}_{P,I,D\_min} + K^1{}_{P,I,D\_opt})}{2} \tag{3.7}$$

Similarly, the upper limit for each parameter is shifted to the interval value of;

$$K^2{}_{P,I,D\_max} = \frac{(K^1{}_{P,I,D\_opt} + K^1{}_{P,I,D\_max})}{2} \tag{3.8}$$

In the Table 3.2, the output data of the Interval Halving Method representing the Range limits, increment and obtained cost and parameters for each iteration.

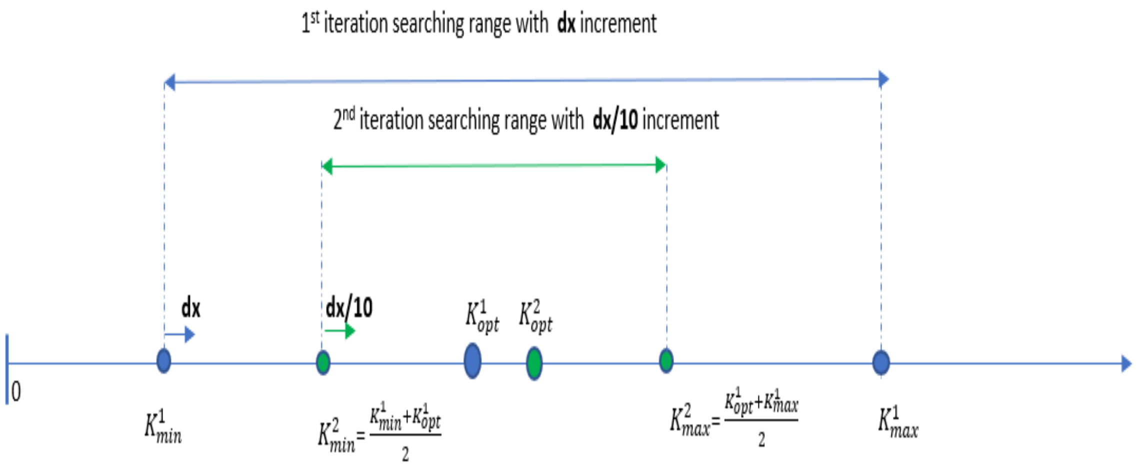

Figure 3.4:Demonstration of Interval Halving Method (IHM).

3.4 System Equations

The plant model for an e-motor is defined for simplicity by considering the input voltage generating desired revolutionary speed. In the following figure,the equivalent DC circuit of the armature and the rotor shaft free-body diagram is shown.

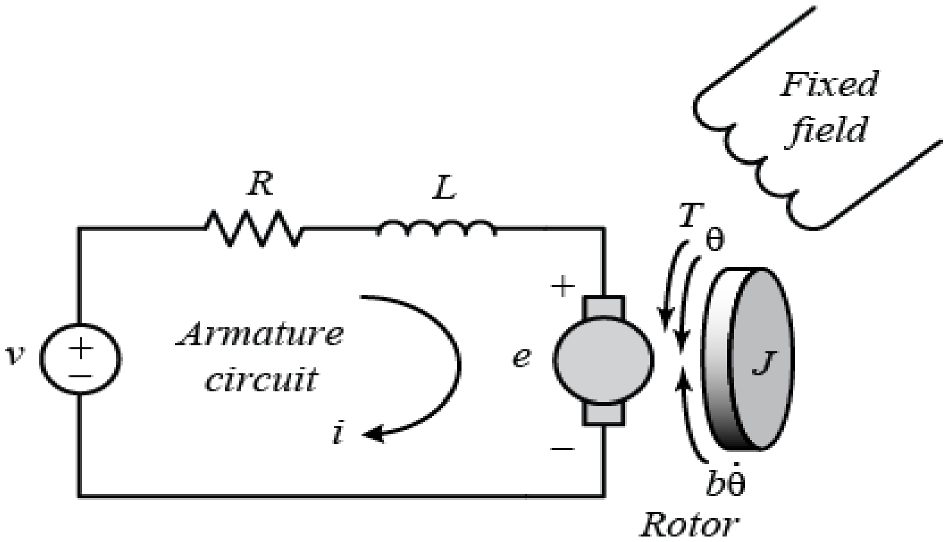

Figure 3.5: Electrical and mechanical circuit of DC motor [28].

The selected brushless DC motor generating torque is proportional to the strength of the magnetic field and the armature current. In this case, the magnetic field is assumed constant. Therefore, the generated motor torque depends on circuit current*i* which is proportional to only input voltage by a constant torque generating factor K_t as shown in the Eq.3.9 and Eq.3.10.

$$U = Ri + L\frac{di}{dt} + K_e\omega \qquad (3.9)$$

$$I\dot{\omega} = K_t i - b\omega \qquad (3.10)$$

K_e is the back-electromotor force constant on the shaft where U is the input voltage, ω is the motor shaft speed in rad/sec,R is the armature resistance, H is the inductance,I is the rotational inertia, b is the friction coefficient and i is the armature current [17].

3.5 Transfer Function

DC motor equations are expressed in terms of Laplace variables by applying appropriate transform as follows;

$$K_t I(s) = \mathrm{s}(\mathrm{Js} + \mathrm{b})\theta(\mathrm{s}) \qquad (3.11)$$

$$U(s) - K_e s\theta(\mathrm{s}) = (Ls + R)I(s) \qquad (3.12)$$

By eliminating the $I(s)$ from two Laplace transform functions above the following open-loop transfer function is obtained by referring armature voltage as input generating shaft rotational speed.

$$G(s) = \frac{\dot{\theta}(s)}{U(s)} = \frac{K_t}{(J.s+b)(L.s+R)+K_e.K_t} \quad [\frac{rad/sec}{V}] \quad (3.13)$$

The e-motor generating thrust force has chosen the following design parameters:

Table 3.1: DC motor design parameters [28].

Motor Parameters	**Value**
Motor armature resistance -R [Ohm]	1
Motor armature inductance-L [Henry]	0.5
Back electro-motor force constant -K_e [V/rad/s]	0.023
Motor torque constant- K_t [N.m/A]	0.023
Motor rotational inertia-I [kg.m^2]	0.01
Motor friction damping coefficient-b [N/rad/s]	0.00003

After inserting the numerical values into the e-motor combinedplant modelfor each input Voltage responds to shaft rotational speed change it has the following transfer function:

$$G(s) = \frac{1}{0.2174s^2+0.43565s+1.0243} \quad (3.14)$$

Since the Proportional Integral Derivative (PID) controller is widely used in control theory, the parameters make the system robust and stable shall be well defined. Now, the model is to be controlled by feeding back transient error $e(t)$ to the controller by selecting proper parametersK_p, K_i and $K_d$as shown in Figure 3.6.

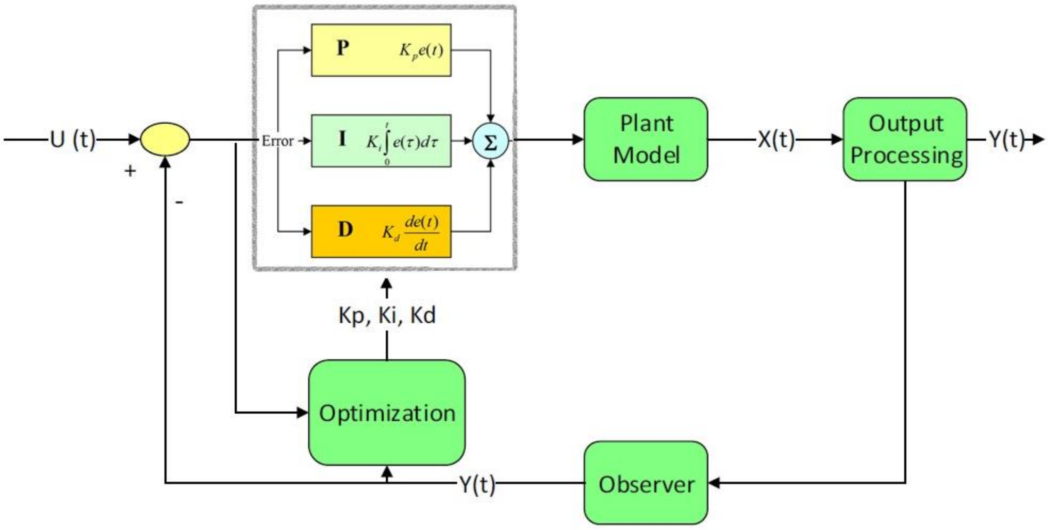

Figure 3.6: Closed-Loop control system with PID controller.

The objective is to search for the optimal control parameters which are the PID coefficients K_p, K_i and K_d [14]. To monitor a range of result for cost function, inputs for K_p, K_i and K_d are evaluated from lower to upper limit by an initial step size of 0.1. The constraints are set by considering the system response based on maximum percentage overshootM_p, rise time T_r and settling timeT_s. The maximum acceptable overshoot M_p to be less than 30%, rise time and settling time to be less than 0.8 sec, 3 sec respectively.

The optimization problem is formed to minimize system performance measure of

$$J = \int_0^{t_f} e(t)^2 dt \tag{3.15}$$

subject to constraints of

$$M_p = 100. e^{\frac{\pi\delta}{\sqrt{1-\delta^2}}} \leq 30 \tag{3.16}$$

$$T_r = \frac{1}{\omega_n}(2.3\delta^2 - 0.078\delta + 1.12) \leq 0.8\, sec \tag{3.17}$$

$$T_s = -\frac{\ln(tolerance)}{\delta\omega_n} \leq 3\, sec \tag{3.18}$$

Here, the system is expected to be closed-loop damped control process oscillation periodically by model input with the natural frequency of ω_n in rad/sec and damping ration of δ varying between 0 and 1.

M_p represents the system aggressiveness.For smooth manoeuvres, M_p is expected not to exceed 30% and J is to be as small as possible, less than 0.5 considerably.

3.6 Implementation

The application of controlling a DC e-motor using Optimal Control Theory is performed by eliminating the error [28] and [29]. The objective function is governed by Linear Quadratic Optimal Control that proposes the following integral form:

$$J = \int e'(t)Qe(t)\, dt \tag{3.19}$$

Where *e(t)* is the error vector between the target state and actual state, *e'(t)* is the transposed vector. Q is positive definite matrix introduced by Ricatti Bellman in 1957 to solve discrete-time optimal control problems for dynamic programming [28]. The cost function for the LQR system written in more compact form by targeting the minimum cost J^* given:

$$J^* = \frac{1}{2} x^{*\prime}(t)P(t)x^*(t) \qquad \text{for t} = [t_i = 0,\ t_f] \tag{3.20}$$

Where, $P(t)$ is the solution of matrix Differential Ricatti Equation and $x^*(t)$ is the closed-loop optimal system solution [28].

The method employed on the motor control system that is given in the previous section multiplied by the PID controller to get a complete closed-loop system transfer function.

$$PID(s) = K_p + K_i \frac{1}{s} + K_d s \tag{3.21}$$

$$G(s) = \frac{1}{0.2174s^2 + 0.43565s + 1.0243} \tag{3.22}$$

$$H(s) = PID(s) * G(s) \tag{3.23}$$

After defining thesearchrange from user input, aset of control parameters for performance measure is assigned to the 3-dimension$J$ matrix.The matrix is dimensioned with three PID parametersK_p, K_i, K_d. For optimal J^*value,the minimum point finder function is used in the loop to obtain $J[K_p , K_i , K_d]$ global minima. Here K_p , K_i , K_d are varying sequentially for each iteration indices. In Figure 3.5 the variation of J with respect to K_p is shown. In Figure 3.6andFigure 3.7 the variation of M_p and T_s with respect to parameters, each surface corresponds to the different value of K_p also can be seen.

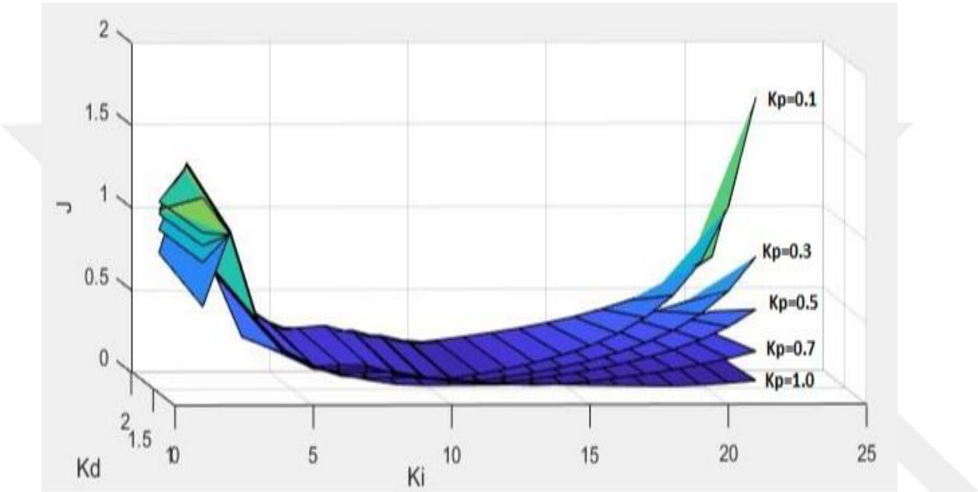

Figure 3.7: Cost function vs. K_p, K_i and K_d.

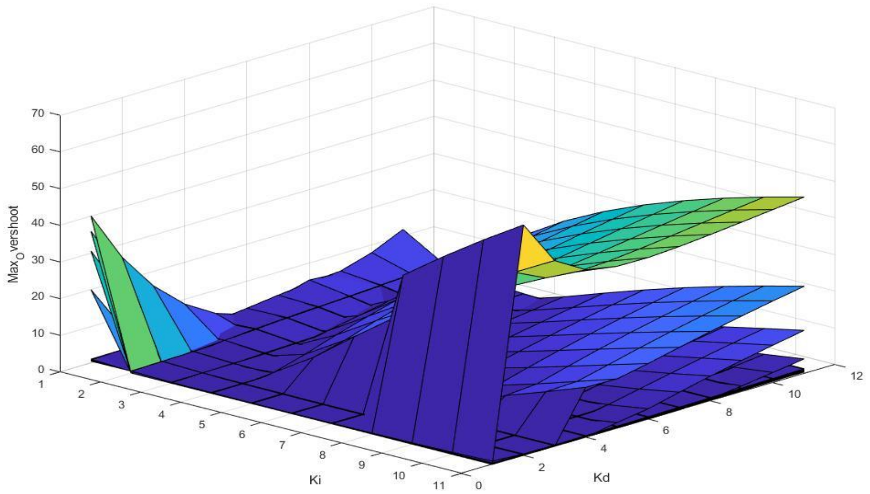

Figure 3.8: Maximum Percentage Overshoot variation withK_i and K_d.

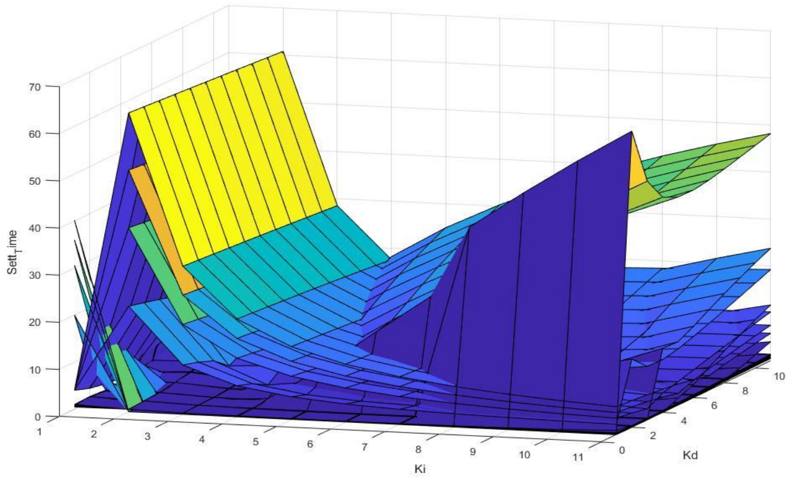

Figure 3.9: Settling Time variation withK_i and K_d.

In Table 3.1, the parameter variation at each iteration step is given. Atthe first iteration, the feasible PID parameters are suggested. Subsequently, the searching range is narrowed down for each iteration loop until the result converged.Accordingly,the parameters upper/lower limits are switched to the next value which to benear the optimal defined at the previous iteration. During each iteration loop, the minimum closed-loop steady-state system erroris squared and integrated to assign$J$.

Table 3.2: Outputs of Interval Halving Method.

Iteration	Kp range [min max]	Kirange [min max]	Kdrange [min max]	Increment	Outputs				
					J^*	Kp_{opt}	Ki_{opt}	Kd_{opt}	Elapsetime [sec]
1	[0 20]	[0 20]	[0 20]	0.1	0.1412	10.00	14.00	2.00	33.57
2	[5 15]	[7 17]	[1 11]	0.01	0.0697	10.00	12.00	6.00	30.89
3	[7.5 12.5]	[9.5 15]	[3.5 8.5]	0.001	0.0686	10.00	13.50	4.00	28.41
4	[8 10.5]	[11.25 13.75]	[1.754.25]	0.0001	0.0686	9.250	12.50	3.00	26.80

3.7 Interpreting the Results

From all the obtained results, the system response is evaluated depending on predefined control parameters. The coefficients obtained from Matlab PID Tuner toolbox are compared with numerically evaluated ones. These values are computed without considering total error and percentage overshoot criteria at the same time. The minimum cost function J, for the tuned controller, is higher than the numerically one. Moreover, the percentage maximum overshoot, M_p, should be less than the defined constraint accordingly. J and M_p are significantly considered as smooth manoeuvres to reach the target point. Below, Table 3.3 and Figure 3.10 compares the performance index between the introduced method and tuner toolbox.

Table 3.3: Control parameters comparison.

Parameters	Tuner Toolbox	Method (ISE)
Kp	0.1457	9.25
Ki	0.7357	12.5
Kd	0	3.0
J	0.1925	0.0686
Mp	0%	4.32%
Tr	inf	1.865s
Ts	5.2422 s	3.167s
Tp	inf	2.486 s

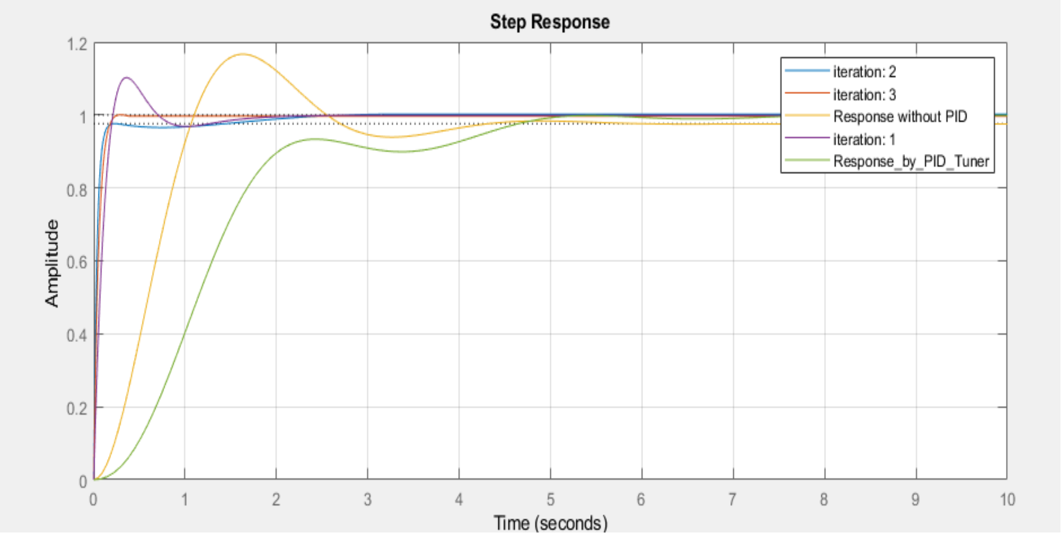

Figure 3.10: System step response at each iteration for optimum K_p, K_i and K_d.

To consider the vehicle smooth and robust manoeuvres,numerically computed parameters introduced by the method are more convenient rather than the toolbox. The minimized cost function is related to the minimum power consumption and minimizing percentage overshoot is related to the smoothness. For a better understanding of how PID parameters are affecting the process output, a trade-off step plots are visualized below for each sequentially K_p, K_i and K_d inputs by 0.1 increments. For small proportional K_p values less than 0.7, the steady-state amplitude is below unity. For K_p=1 and K_p=1.1 a cumulative range of plots are expressed by varying K_i between 0.0 and 1.0. Nevertheless, K_d is zero since it has a small effect on the PID controller and cost computation time [22].

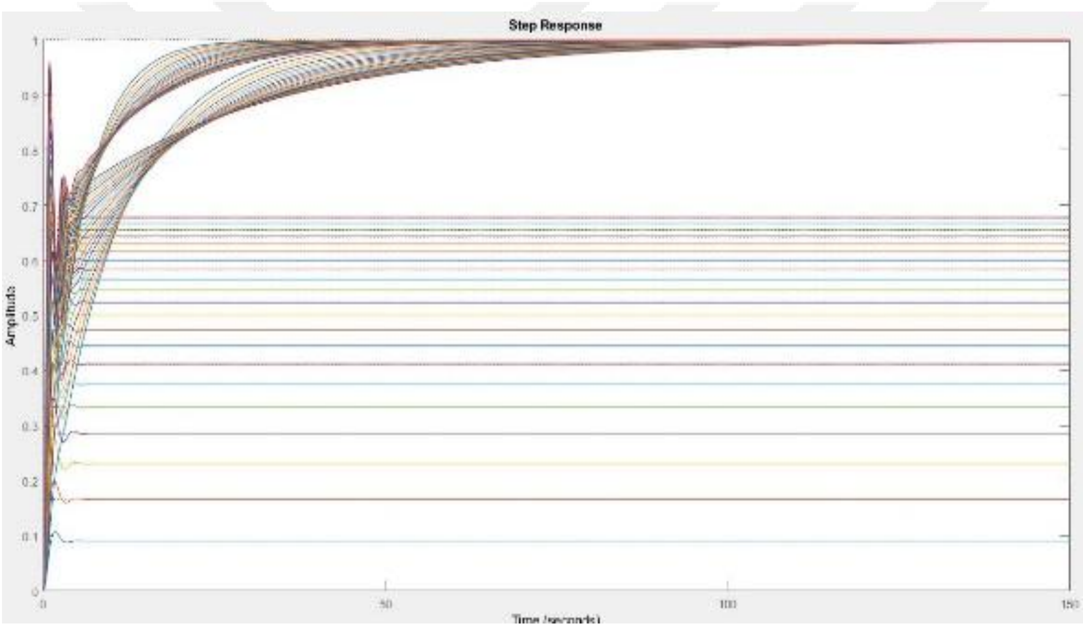

Figure 3.11:A trade-of step plots.

3.8 Application for Future Work

Since the E-VTOL kinematic equations are governed based on the only DC motor mechanical, electrical and desired shaft speed, the complete vehicle complete dynamic model is roughly estimated achieved to see a response. The e-motor plant model is used to derive E-VTOL thrustmodel including take-off cruise performance. The absence of rolling and yawning control may lead to rough estimation since there is no decoupling of attitude control. For precise computation, the range of sequential inputs can be narrowed down in the loop with slight tolerance just after optimal function obtained the global minima.

4. CONCLUSIONS AND RECOMMENDATIONS

4.1 Practical Application of This Study

The thesis contributes to the research and developments of electrification of aerial vehicles by providing a feasible range of electric aircraft design methodology. It explains the mainconstraints through design phases and determines the key parameters for energy requirements as well as optimization of the e-motor control system parameters used in its powertrain. By defining the instantaneous minimum power requirement during level flight, the mass portion of total aircraft weights is estimated and the optimum design range is provided. One can cascade the design parameters from the equations of motions and then determine the average range/flight endurance with the help of the first method. From the second method, an online optimization search algorithm is introduced to make a control system PID parameters more tuned. Since the PID controller is widely used in the application, a robust system can be achieved by tuning control parameters instantaneously. The second method performs the parameters tuning by narrowing down search range after each iteration. This enables the objective function convergence after certain steps. While reaching the global minima objective cost function, the value convergences a predefined threshold, the corresponding PID parameters are deployed in the control system to make manoeuvres smooth and robust.

4.2 Conclusion

In this thesis, two comprehensive methods are proposed for electric aircraft design and control parameters optimization. From the first method, a general comparison of design parameters isgraphically presented to oversee a high-level relation of flight endurance time versus maximum take-off weight, battery weight versus maximum take-off weight and total range depending on power consumption. The method proposes the parameters optimization for future electric aerial vehicles by determining the feasible conceptual design range. Parameters used in kinematic equations are critically enrolled for the optimization problem. The main objective is to equate the total energy required through flight profile and sustain instantaneous power consumption of the propulsion unit by an integrated battery on vehicle. The method employs the consumed energy for the vehicle kinetic energy and drag force work are done by sweeping aircraft cross-sectional area aerodynamically. Comparing two different aircrafts demonstrates the key role of total vehicle mass requiring total battery weight to overcome targeted flight time. By introducing the range and endurance equations, the parameters that to be maximized or minimized are in the definite scope.

The second method proposes the recent approach to tune control parameters in parallel calculation of the e-motor drive system, which is used as the propulsive component in the powertrain. PID coefficients are optimized in online search by considering the minimum integral squared error objective function. The cost function is minimized by obeying system constraints which are rise time, settling time and maximum percentage overshoot. A search criterion is set before the algorithm run and set of feasible PID parameters stored for each iteration. The search interval is sequentially halved after each iteration which enhances the result accuracy. Therefore, the method is called Interval Halving Search Method (IHSM) by switching upper and lower bound to the near region of previously obtained optimal coefficients. In this case, the constrains those set for maximum overshoot, settling time and rise time are obeyed in the dynamic optimization model. Error is profoundly eliminated by suggesting a set of PID coefficients for an e-motor transfer function. Search loop excited when the error converges to a predefined threshold. To consider vehicle smooth and robust manoeuvres of the vehicle, numerically computed parameters are introduced by a method more convenient than those obtainedfrom Matlab Tunertoolbox. The minimized cost function is related to the minimum power consumption and minimizing percentage overshoot is related to the smoothness.

4.3 Recommendation

With this comprehensive thesis study, two practical methods and a recent literature survey are proudly presented for future air mobility. Considering the zero-emission air transportation, an initiative decision, endeavour me to study on this topic and I am glad to demonstrate my approach by this thesis to be a part of the clean air transport journey. From the past decade up to now, several design methodologies have been proposed for fully electrified short-range aircrafts (UAVs, e-VTOLs) and hybrid long-range domestic aeroplanes. With this study, at least in national civil air transportation, there will be a record of literature electric aircraft design approach end two unique methods for future work. As a self-criticism, it can be honestly notified that the calculations and estimations are performed roughly. However, both methods are verified by simulation algorithm by asoftware tool. For the next step, one can enhance the optimization model implemented in a control system to get results at an optimum level. Even the first method, which is the proposal of design parameters for extended range and endurance, can be extendedfor concrete design parameters by governing all vehicle dynamic equations and stability equations (i.e. 6-Degree of Freedom Stability model).

REFERENCES

[1]**Markets&Markets.** (2019). Fixed-wing VTOL UAV Market by Vertical (Military, Government & Law Enforcement, Commercial), Propulsion (Electric, Hybrid, Gasoline), Mode of operation (VLOS, EVLOS, BVLOS), Endurance, Range, MTOW, and Region - Global Forecast to 2030.

[2]**Michele, R.** (2014).Contributionsto Aircraft Preliminary Designand Optimization,Preliminary Sizing – *Matching Charts, Aerospace EngineeringTraining Session*.

[3] **Url-1** <*https://www.rolls-royce.com/media/press-releases/2019/19-12-2019-rr-unveils-all-electric-plane-targeting-the-record-books.aspx*>,dateretrieved 04.02.2020.

[4]**Riboldi, C.E., Gualdoni F. &Trainelli, L.** (2018). Preliminary Weight Sizing of Light Pure-Electric and Hybrid-Electric Aircraft,*Transportation Research Procedia, Vol. 29, 2018, pp. 376-389.*

[5] **Bacchini, A. &Cestino, E.** (2019). *Electric VTOL Configurations Comparison. Department of Mechanical and Aerospace Engineering,*Politecnico di Torino, Turin, Italy.

[6] **Rohacs, J. &Rohacs, D. (**2018). *Effect of Energy Balance Evaluation on Conceptual Design of Electric and Hybrid Aircraft,* Budapest University of Technology and Economics, Budapeşt, Hungary.

[7]**Rohacs, J. &Rohacs, D. (**2018). List of electric aircraft, ADS1884-44 (retrieved on 18.04.2018).

[8] **Henningson, P. &Hedenström, A.** (2010). *Aerodynamics of Gliding Flight in CommonSwifts*, Department of TheoreticalEcology, Lund University,Lund, Sweden.

[9] **Bonni, J., Burghoff B., Dincer E. et all.** (2017). *Conceptual Design of a LowNoiseHybridPassenger Aircraft*, RWTH AachenUniversity, Aachen, Germany.

[10] **Deshpande, M. D., Sivapragasam, M**. (2017). *How Do Wings Generate Lift?,* Ramaiah University, India.

[11] **Ibraheem, K. & Abdul-Adheem, R.** (2017). *From PID to Nonlinear State Error Feedback Controller,* College of Engineering, Baghdad University, Baghdad, Iraq.

[12] **Kirk, D.E.**(1970).*Optimal Control TheoryandIntroduction*, PrenticeHall, New Jersey.

[13]**Nikowitz, M.**(2016). *Advanced HybridandElectricVehiclesSystemOptimizationandVehicle Integration,*Springer, Vienna, Austria.

[14] **Wang, Y.S.**(2017). *A System Level Approachto Optimal Controller Design forLarge-Scale Distributed Systems,* California Institute of Technology.

[15] **Leong**,**Y.L.** (2017). *Optimal Controller SynthesisforNonlinearSystems*, California Institute of Technology.

[16**] Nieto, S.G. et al**. (2019). *Motion EquationsandAttitude Control in theVertical Flight of a VTOL Bi-Rotor UAV*.

[17] **Baldursson**,**S.** (2005).*BLDC Motor Modellingand Control – A Matlab®/Simulink® Implementation*.

[18]**Muraoka, K.et al**. (2009).*Quad-TiltWingVTOL UAV: AerodynamicCharacteristicsandPrototype Flight Test*. Japan Aerospace Exploration Agency, AIAA Infotech,Tokyo, Japan.

[19] **Zou, L. et al.** (2017).*Imaged-Based Visual Servo Control for a VTOL Aircraft*. Mathematical Problems in Engineering Volume: 2017, ID 4806769.

[20]**Hauser, J. et al**. N*onlinear Control Design forSlightlyNon-minimum PhaseSystems.*Applicationto V/STOL Aircraft, Automatica Vol:28 No:4.

[21] **Staples, G.**PropellerStatic&DynamicThrustCalculation, 2013, retrievedfrom: <*https://www.flitetest.com/articles/propeller-static-dynamic-thrust-calculation*>, date retrieved: 15.07.2019.

[22**] Hystad**, **A.V. (**2015). Model, designand Control of a Quadrocopter, NorwegianUniversity of ScienceandTechnology.

[23] **Corrigan**, **D. (**2012). CharacterisingtheResponse of a Closed-LoopSystem, TrinityCollege Dublin.

[24] **Sharaf, A. M. &El-Gammal**, **A. A.** *An IntegralSquaredError -ISE Optimal ParametersTuning of Modified PID Controller forIndustrial PMDC Motor Based on ParticleSwarmOptimization-PSO*, CentreforEnergySystems, University of Trinidad and Tobago UTT.

[25] **Url-2<***https://www.space.com/16623-first-powered-airship.html*>, retrieved date 10.11.2019.

[26] **Jacob, S. et al**. (2017).*Hybrid-Electric Propulsion Integration in Unmanned Aircraft*, RMIT University, Melbourne, Australia.

[27] **MIT unified Lecture Notes**, The Breguet Range Equation<*http://web.mit.edu/16.unified/www/FALL/thermodynamics//notes/node98.html*>retrieved date 10.03.2020.

[28]**Tomy M.,& Thosar, A.G.***Optimal Control of DC Motor using Linear Quadratic Regulator*. Government Engineering College, Aurangabad, India.

[29] **Petrov, U.P.** (1971).*Optimum Control of the Electric Drive Taking into Account the Limitations on Heating- Cracateristic of Electric Drive*. Leningrad.

[30] **Clean Aviation**.(2020). *The proposed European Partnership on Clean Aviation*. Strategic Researchand Innovation Agenda, Paris.

[31] **Bushnell, D. M.** (2018). *Enabling Electric Aircraft_Applications and Approaches*. Langley Research Center, Hampton,Virginia.

[32]**Secrtariat of ICAO.** (2019).*Electric, Hybrid, and HydrogenAircraft – State of Play*.Climate Change Mitigation: Technology and Operations, ICAO.

[33] **Skyhawk**, (1978*). Pilot's Operating Handbook, CESSNA Model 172N*, CESSNA Aircraft Company, Kansas, USA.

[34]**Url-3**<*http://www.team.aero/files/topics/60.pdf*>, retrieved date: 25.06.2020.

APPENDICES

APPENDIX A: Scripts (CtrlOpt_V5_Method_PID.m)

```
%%PID Parameters Optimization by Interval Halving- Integral Squared
Method
close all
clear;
clc;

s= tf('s');
%G=input('Please transfer function nomunator');
G= 1/(0.2174*s^2 + 0.43565*s + 1.0243); %Transfer Function of Plant
%G= 1/(s^2 + 0.5*s + 0.1);
PID_tuner= 0.1457 + 0.7357/s + 0*s;

Response_by_PID_Tuner=feedback(G*PID_tuner,1);

Kp_min= input('Enter the Kp min value=');  %Searcing range for
Proportional Coefficient,Kp
Kp_max= input('Enter the Kp max value=');
Ki_min= input('Enter the Ki min value=');  %Searcing range for
Integral Coefficient,Ki
Ki_max= input('Enter the Ki max value=');
Kd_min= input('Enter the Kd min value=');  %Searcing range for
Derivative Coefficient,Kd
Kd_max= input('Enter the Kd max value=');

epsilon= 0.001;     %Error value of seraching termination
J_accept_tol= 0.5; %Maximum admissible error tolerance
iter1= 1;
%Mp_accept_tol= 0.3;
%iter2= 1;
dx= (Kp_max - Kp_min)/10; %Kp resolution
x= [Kp_min:dx:Kp_max]; % Kp rangelentgh
dy= (Ki_max - Ki_min)/10; %Ki resolution
y= [Ki_min:dy:Ki_max]; % Kirangelentgh
dz= (Kd_max - Kd_min)/10; %Kd resolution
z= [Kd_min:dz:Kd_max]; % Kd rangelentgh


%% First trial to find optimum PID parameters
for i=1:numel(z)
    Kd(i) = Kd_min + i*dz;
for j=1:numel(y)
Ki(j) = Ki_min + j*dy;
for k=1:numel(x)
Kp(k) = Kp_min + k*dx;

if   Kp(k) == 0 &&Ki(j) == 0 && Kd(i) == 0
                     PID(i,j,k) = 1.0 ;
else
PID(i,j,k) = Kp(k) + Ki(j)/s + Kd(i)*s;
end

O_loop=step(G);
H=feedback(G*PID(i,j,k),1);
C_loop=step(H);
```

```
                 dt=0.01;
t=0:dt:10;

error=1-C_loop;
[wn,zeta] = damp(H); %Wn:natural frequency in rad/sec; zeta: damping
ratio
                 Zeta=zeta(1);
Wn=wn(1);
                 fi=acos(Zeta); %phase shift angle
Wd=Wn*sqrt(1-Zeta*Zeta); %damped frequency in rad/sec
                 Td=(1+0.7*Zeta)/Wn;    %Delay time
                 Tr=(pi-fi)/Wd;  %Rise time, reaching 90% of target
level
Tp=pi/(Wd);    %Peak time, overshoot reached instant
                 Mp=100*2.718^(-1*((Zeta*pi)/sqrt(1-Zeta^2)));
%Percentage overshoot
                 Ts=4/(Zeta*Wn);  %Settling time

Nat_Freq(i,j,k)= Wn;
Damp_Ratio(i,j,k)= Zeta;
Rise_Time(i,j,k)= Tr;
Peak_Time(i,j,k)= Tp;
Max_Overshoot(i,j,k)= Mp;
Sett_Time(i,j,k)= Ts;

%ITAE
                 J(i,j,k)=sum(abs(error+error)*dt);

ifJ_accept_tol> J(i,j,k) && J(i,j,k)> 0 %% constraints can be added
Jopt(iter1) = J(i,j,k);
KpOpt_J(iter1)=Kp(k);
KiOpt_J(iter1)=Ki(j);
KdOpt_J(iter1)=Kd(i);
indexKd(iter1) = i;
indexKi(iter1) = j;
indexKp(iter1) = k;
                     iter1 = iter1 + 1;
end


end

end

end

[J_MinCost, MinCost_iter] = min(Jopt(1,:));
KpBest_J = KpOpt_J(MinCost_iter);
KiBest_J = KiOpt_J(MinCost_iter);
KdBest_J = KdOpt_J(MinCost_iter);
JoptPosition = [indexKd(MinCost_iter); indexKi(MinCost_iter);
indexKp(MinCost_iter)];

disp('iteration=1')
disp('First min J:')
J_MinCost
disp('First feasible PID, [Kp, Ki, Kd]:')
[KpBest_J, KiBest_J, KdBest_J]
```

```
M=feedback(G*(KpBest_J + KiBest_J/s + KdBest_J*s),1);


%End of First trial to find optimum PID parameters
%%

%% Optimizing parameters by Interval Halving method
count=1;
lgnd_text={};
whileJ_MinCost> epsilon

tic
Kp_min = (Kp_min + KpBest_J)/2;
Kp_max = (Kp_max + KpBest_J)/2;
Ki_min = (Ki_min + KiBest_J)/2;
Ki_max = (Ki_max + KiBest_J)/2;
Kd_min = (Kd_min + KdBest_J)/2;
Kd_max = (Kd_max + KdBest_J)/2;

        dx= (Kp_max - Kp_min)/10; %Kp resolution
        x= [Kp_min:dx:Kp_max]; % Kp rangelentgh
        dy= (Ki_max - Ki_min)/10; %Ki resolution
        y= [Ki_min:dy:Ki_max]; % Kirangelentgh
dz= (Kd_max - Kd_min)/10; %Kd resolution
        z= [Kd_min:dz:Kd_max]; % Kd rangelentgh

count= count+1;
        str=['iteration=', num2str(count)];
disp(str)

for i=1:numel(z)
Kd(i) = Kd_min + i*dz;
for j=1:numel(y)
Ki(j) = Ki_min + j*dy;
for k=1:numel(x)
Kp(k) = Kp_min + k*dx;
PID(i,j,k) = Kp(k) + Ki(j)/s + Kd(i)*s;
O_loop=step(G);
H=feedback(G*PID(i,j,k),1);
C_loop=step(H);

                 dt=0.01;
t=0:dt:10;

error=1-C_loop;
[wn,zeta] = damp(H); %Wn:natural frequency in rad/sec; zeta: damping
ratio
                 Zeta=zeta(1);
Wn=wn(1);
                 fi=acos(Zeta); %phase shift angle
Wd=Wn*sqrt(1-Zeta*Zeta); %damped frequency in rad/sec
                 Td=(1+0.7*Zeta)/Wn;   %Delay time
                 Tr=(pi-fi)/Wd;  %Rise time, reaching 90% of target
level
Tp=pi/(Wd);    %Peak time, overshoot reached instant
                 Mp=100*2.718^(-1*((Zeta*pi)/sqrt(1-Zeta^2)));
%Percentage overshoot
                 Ts=4/(Zeta*Wn);  %Settling time
```

```
Nat_Freq(i,j,k)= Wn;
Damp_Ratio(i,j,k)= Zeta;
Rise_Time(i,j,k)= Tr;
Peak_Time(i,j,k)= Tp;
Max_Overshoot(i,j,k)= Mp;
Sett_Time(i,j,k)= Ts;

%ITAE
                 J(i,j,k)=sum(abs(error)*dt);

ifJ_accept_tol> J(i,j,k)  && J(i,j,k)> 0 %% constraints can be added
Jopt(iter1) = J(i,j,k);
KpOpt_J(iter1)=Kp(k);
KiOpt_J(iter1)=Ki(j);
KdOpt_J(iter1)=Kd(i);
indexKd(iter1) = i;
indexKi(iter1) = j;
indexKp(iter1) = k;
                     iter1 = iter1 + 1;
end


end

end

end

[J_Min, MinCost_iter] = min(Jopt(1,:));
KpBest_J = KpOpt_J(MinCost_iter);
KiBest_J = KiOpt_J(MinCost_iter);
KdBest_J = KdOpt_J(MinCost_iter);
JoptPosition = [indexKd(MinCost_iter); indexKi(MinCost_iter);
indexKp(MinCost_iter)];

Kp_optimum= (Kp_min + Kp_max)/2;
Ki_optimum= (Ki_min + Ki_max)/2;
Kd_optimum= (Kd_min + Kd_max)/2;

E(count)=J_Min;

disp('Optimum/minimum J value:')
            E(count)
disp('Optimum [Kp, Ki, Kd] Values:')
            [Kp_optimum, Ki_optimum, Kd_optimum]

Kp(count)=Kp_optimum;
            Ki(count)=Ki_optimum;
Kd(count)=Kd_optimum;
            toc

if E(count)== E(count-1)
disp('End of Session. Cost function J,total error converged!')
                E(count)
break
end
```

```
CTRL(count)= Kp(count)  + Ki(count)/s + Kd(count)*s;
             R(count)=feedback(CTRL(count)*G,1);
             step(R(count)), grid on

lgnd_text{count-1}= ['iteration: ', num2str(count)];

             hold on

end

%% Plotting the responses
lgnd_text{count-1}='Response without PID';
lgnd_text{count}= 'iteration: 1';
step(G)
hold on
step(M)

legend(lgnd_text)

%%Copyright: IBRAHIM CICEK, Istanbul Technical University, January
2020.
```

CURRICULUM VITAE

Name Surname : **Ibrahim CICEK**

Place and Date of Birth : **05.05.1993**

E-Mail : **cicekib@itu.edu.tr**

cicekib@gmail.com

EDUCATION :

- B.Sc.2017, Istanbul Technical University, Faculty of Aeronautics and Astronautics, Aeronautical Engineering Department

PROFESSIONAL EXPERIENCE:

- 2020-Present, FEV Turkey, xCU& Power Electronics Department, Electric Vehicle Systems Engineer
- 2018-2020, AVL Turkey Research & Development Center, THC/SYS, Hybrid &Electric Vehicle System Development, Systems Engineering.
- 2016, Freebird Airlines, Organization Management Intern, Technical Documentation
- 2014, ITU GK/BBY, Community Volunteer

PUBLICATIONS, PRESENTATIONS:

- **Cicek,İ., NikbayM.,** 2020: Optimization of E-Motor Control Parameters for ElectricallyPropelled Vehiclesby Integral Squared Method, ICMIMEA 2020 :22th Int. Conf. on Mechanical, Industrial and Mechatronics Engineering Applications
- **Cicek,İ., NikbayM.,** 2019: Optimization of Control Parameters for an Electrified Vertical Take-off Landing Vehicle Using the Integral Squared Method, CM4PEccomas Thematic Conference -Computational Methods in Multi-Scale, Multi-Uncertainity and Multi-Physics Problems, July 15-17, Porto, Portugal.
- **Medet, O., Cicek, İ., Gülmez, M.** 2016. ITU Hurguc Team- Conceptual Design of Turboprop Engine Final Report,*AIAA Undergradute Team Engine Design Competition.*
- **Cicek,İ., Kayayurt, S.** 2017. Üniveristeler İçin Temel Fizik.